Geological Survey of Finland

Bulletin 344

Metamorphic zones and the evolution of granulite grade metamorphism in the early Proterozoic Pielavesi area, central Finland

by
Pentti Hölttä

Geologian tutkimuskeskus
Espoo 1988

Geological Survey of Finland, Bulletin 344

METAMORPHIC ZONES AND THE EVOLUTION OF GRANULITE GRADE METAMORPHISM IN THE EARLY PROTEROZOIC PIELAVESI AREA, CENTRAL FINLAND

by

PENTTI HÖLTTÄ

GEOLOGIAN TUTKIMUSKESKUS
ESPOO 1988

Vammala 1988. Vammalan Kirjapaino Oy

Hölttä, P., 1988. Metamorphic zones and the evolution of granulite grade metamorphism in the early Proterozoic Pielavesi area, central Finland. *Geological Survey of Finland, Bulletin 344.* 50 p., 22 figures, 19 tables.

The rocks of the Pielavesi area, which borders an Archaean craton, have been divided into six fault bounded blocks that differ in pressure and temperature conditions, ranging from amphibolite to granulite facies. In addition, metamorphic zoning attributable to contact effects has developed in the vicinity of mangerite intrusions.

The PTt path has been studied for the granulite facies Pielavesi block with the aid of mineral reactions, and geothermobarometers. The garnet-, cordierite- and orthopyroxene-bearing gneisses in the Pielavesi block exhibit abundant corona textures. The reactions observed include: opx + pl = grt + qtz, opx + crd = grt + qtz, opx + ts = grt and pl + iron oxide = grt. Textural data indicate, that these reactions have proceeded in both directions in the same rocks.

Metamorphism culminated at a temperature of 800—880°C and at a pressure of 5.5 ± 1 kb.

Results obtained with the GRIPS barometer and the garnet-ilmenite thermometer based on the compositions of plagioclase and ilmenite inclusions in a large garnet grain imply that cooling following the culmination of the metamorphism was almost isobaric. This was succeeded by a rise in temperature, which was in turn followed by almost isobaric cooling once again. The garnet coronas developed around orthopyroxenes during isobaric cooling. During the subsequent uplift, orthopyroxene coronas developed around the garnet. Titanite ages show that cooling down to 400—450°C took place ca. 1860 Ma ago.

Key words: metamorphism, P-T conditions, PTt path, mineral composition, granulites, Proterozoic, Pielavesi, Finland

P. Hölttä, Geological Survey of Finland, 02150 Espoo, Finland.

This paper is a contribution to IGCP project 235 (Metamorphism and Geodynamics)

ISBN 951-690-306-1
ISSN 0367-522X

CONTENTS

Introduction 5
Metamorphic zones and geological setting of the area 5
Block I, Vieremä 9
Block II, Lampaanjärvi 10 10
Block III, Pielavesi 12
Block IV, Osmanki 12
Block V, Korppinen 12
Block VI, Pihtipudas 13
PT determination 14
Chemical data for minerals 14
Thermobarometry 15
PTt evolution of the Pielavesi granulite block 22
Petrography and mineral reactions 23
Mineral chemistry 29
Orthopyroxene 29
Garnet 29
Cordierite 32
Biotite 32
Plagioclase 32
Orthoamphibole 32
Spinel 33
Iron oxides 33
PT determinations 33
Ilmenite and plagioclase inclusion in garnet 40
Age determinations 43
PTt evolution 44
Discussion 46
Acknowledgements 47
References 47
Appendix: Map coordinates of sample localities

METAMORPHIC ZONES AND THE EVOLUTION OF GRANULITE GRADE METAMORPHISM IN THE EARLY PROTEROZOIC PIELAVESI AREA, CENTRAL FINLAND

by
PENTTI HÖLTTÄ

INTRODUCTION

The rocks of the Pielavesi area belong to the Svecofennidic orogenic belt of eastern Finland. The main features of metamorphism of this belt have been discussed by Korsman *et al.* (1984), who concluded that the Svecofennidic orogeny can be divided into at least three stages. At the margin of the Archaean craton strong contact metamorphism was associated with the emplacement of the 1890 Ma old granitoids. Some gneissose granitoids have yielded an even older age, 1930—1920 Ma, suggesting an earlier crust-forming process. The metamorphism in the migmatite zone of southern Finland is characterized by relatively late culmination, 1840—1810 Ma ago.

The metamorphism of the craton margin (Pielavesi area) differs from that of the migmatite zone of southern Finland in both type and time. In the granulite areas of southern Finland, metamorphism reached culmination at low pressures, c. 3—6 kb, (Korsman *et al.*, 1984; Schreurs and Westra, 1986; Hölttä, 1986), the metamorphic grade increasing progressively towards the granulite areas (Korsman, 1977). The granulites at the margin of the craton are bounded by faults, and the peak of metamorphism was reached earlier and at pressures higher than in the granulites of southern Finland, the last thermal pulse being due to the 1890 Ma old mangerite intrusions.

The present work seeks to establish the metamorphic zones of the Pielavesi area, (Fig. 1), to study their PT conditions with thermobarometers, and to delineate the PT evolution with the aid of metamorphic reactions and mineral compositions, the emphasis being on the granulite block.

METAMORPHIC ZONES AND GEOLOGICAL SETTING OF THE AREA

The study area (Fig. 1) covers the 1 : 100 000 map sheets of Pielavesi, Kiuruvesi, Pyhäsalmi and Pihtipudas. The results of geological mapping have been published for the map sheets of Pihtipudas, Pielavesi (Salli, 1969, 1977, 1983) and Kiuruvesi (Marttila, 1977, 1981).

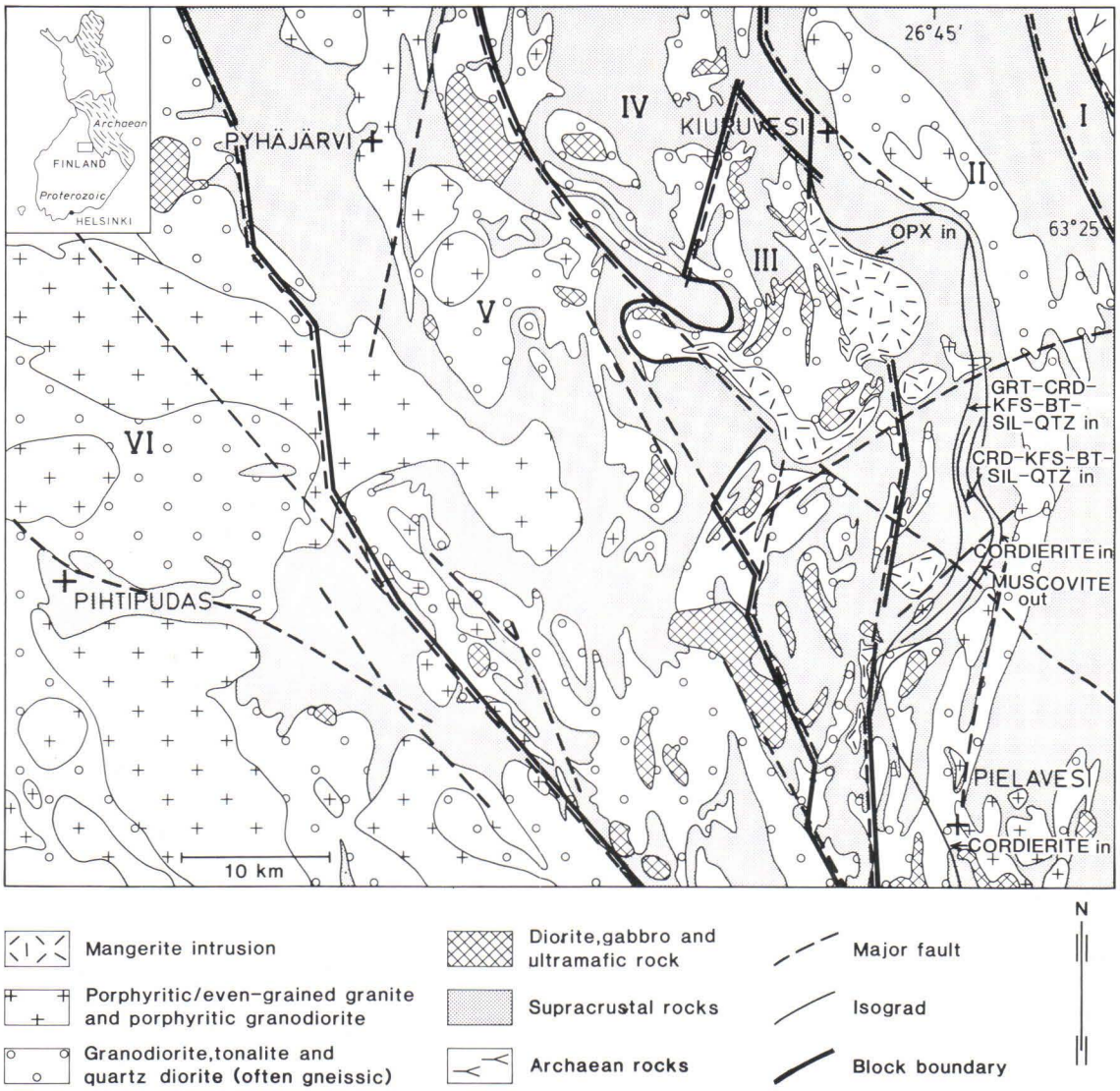

Fig. 1. Metamorphic map of the Pielavesi area. Geological base map simplified from the map of Kuosmanen (1988). Some of the faults on the map are based on field observations, and some on the interpretation of geophysical data by Kuosmanen (op. cit.). The metamorphic blocks are: I Vieremä, II Lampaanjärvi, III Pielavesi, IV Osmanki, V Korppinen and VI Pihtipudas (see text).

The area of the present study is divided into six metamorphic blocks on the basis of metamorphic grade. From the margin of the craton westwards they are: I Vieremä, II Lampaanjärvi, III Pielavesi, IV Osmanki, V Korppinen and VI Pihtipudas (Fig. 1). The blocks also differ from each other in lithology and are separated by strike-slip faults; it is for this reason that the term metamorphic block is used. The classification of the blocks is based on the appearance or disappearance of certain index minerals in peraluminous supracrustal rocks. This often coincides

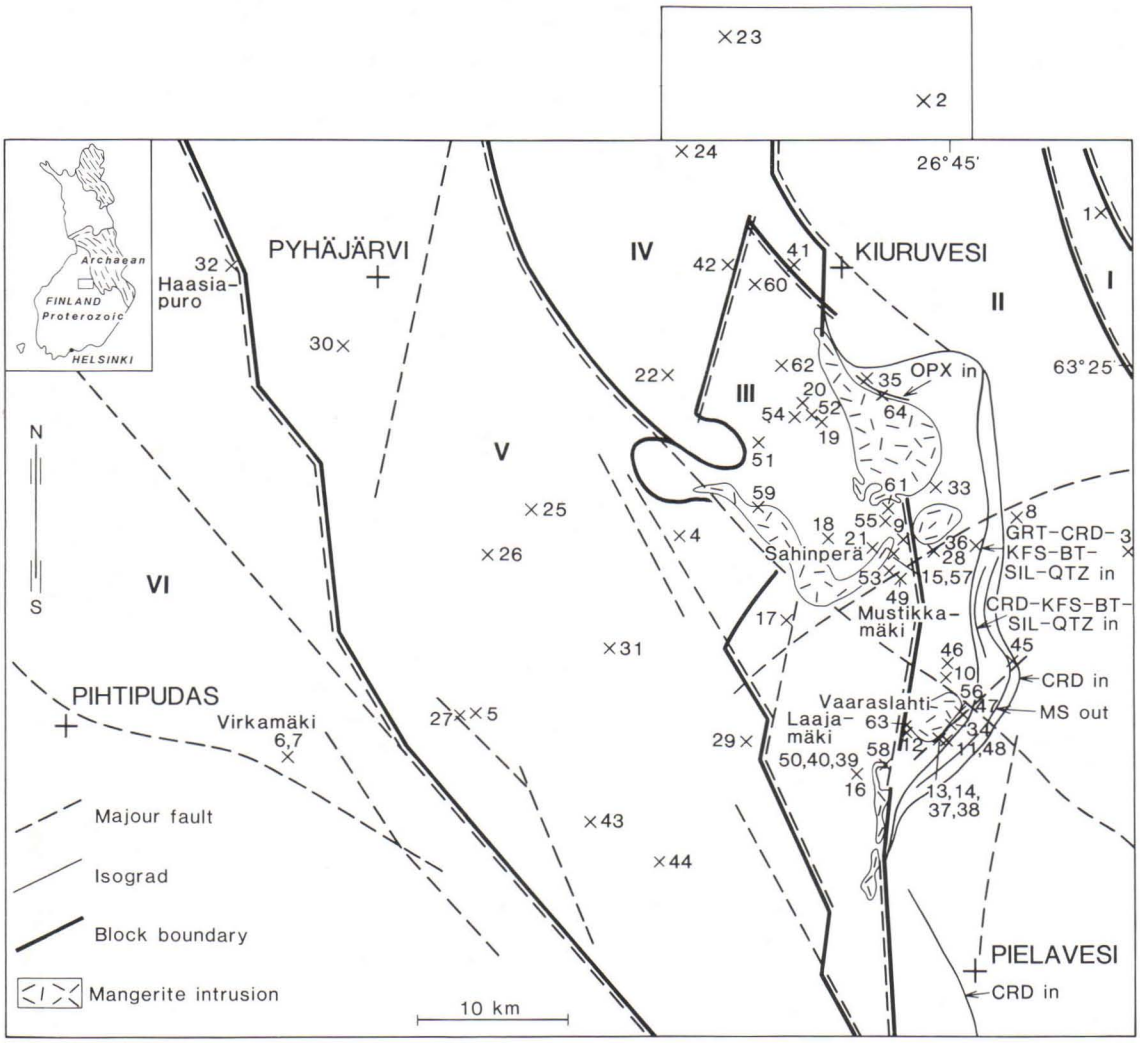

Fig. 2. Location of the samples with analytical data given in Tables 3—17.

with block boundaries, but the Lampaanjärvi block also exhibits metamorphic zoning due to the emplacement of mangerite (coarse-grained hypersthene monzonite) intrusions. Table 1 shows characteristic mineral assemblages in the blocks. Intense retrograde hydration reactions are typical of the whole margin of the craton, and Table 2 lists some of the retrograde reactions observed in the blocks. The abbreviations used in the tables and in the text are according to Kretz (1983).

The blocks of Vieremä, Lampaanjärvi and Pihtipudas constitute clearly distinct units in terms of lithology, whereas the blocks of Pielavesi, Osmanki and Korppinen have several features in common. The Vieremä block is composed predominantly of mature and immature sedimentary rocks: conglomerates, quartz sandstones, quartzites, quartz wackes and greywackes. The sedimentary rocks in the Lampaanjärvi block are mainly aluminous turbiditic metapelites whose primary structures have largely

been destroyed by metamorphism and deformation but which in places show features suggestive of graded bedding and load cast structures. The volcanics of the Lampaanjärvi block constitute a series from felsic to mafic rocks. The features that the Pielavesi, Osmanki and Korppinen blocks have in common are garnet-cordierite-orthopyroxene/orthoamphibole rocks which were originally hydrothermally altered (Fe-Mg-rich, alkali-deficient) volcanics, predominantly bimodal volcanism, limestones and massive Cu-Zn ores (Huhtala, 1979); the latter have not been encountered in the other zones. In the Osmanki and Korppinen blocks the mica gneisses are potassium feldspar-deficient, often migmatitic rocks. Gneissose granitoids are very common. The mica gneisses in the granulite zone are nebulitic migmatites. On the borders of the Pielavesi zone there are several mangerite intrusions of the 1890 Ma age group (Salli 1983). Within the block there are norites, gabbros and diabases of the same age (Marttila 1981); most of the plutonic rocks are, however, pyroxene-bearing intrusives that show textural lineation and vary from tonalite to diorite in composition. The Pihtipudas block is mainly composed of felsic, intermediate and mafic plutonics and volcanics that are richer in potassium than those in the Korppinen area. Pelitic rocks are rare at Pihtipudas.

The metamorphic structure of the area is related to tectonic evolution. Pajunen (1986) studied deformation in the Tervo area, south of Pielavesi, and came to the conclusion that regional metamorphism was associated with the early D_a deformation phase. The D_a structures are cut by a strong fault deformation, D_b. The area also exhibits strong N-S striking faulting, which Pajunen (op. cit.) termed Dd.

According to Ward (1988), the trend of the early deformation phases (1 and 2) in the Pielavesi area coincides with the lithological layering. At a later stage (phases 3, 4 and 5), the earlier structures became reoriented. The third deforma-

Table 1. Characteristic mineral assemblages of the peraluminous rocks in the metamorphic blocks of the Pielavesi area.

Block I, Vieremä	Block II, Lampaanjärvi	Block III, Pielavesi	Block IV, Osmanki
st-bt-ms-qtz ± sil	bt-ms-pl-qtz ± sil ± grt	bt-grt-pl-qtz ± cum	bt-crd-grt-sil-pl-qtz
grt-bt-ms-pl-qtz	crd-bt-sil-pl-qtz	bt-opx-kfs-pl-qtz	bt-crd-sil-qtz
	bt-sil-kfs-pl-qtz	bt-grt-kfs-pl-qtz ± hc	bt-grt-cum-pl-qtz
	bt-sil-crd-kfs-pl-qtz	bt-crd-grt-kfs-pl-qtz	bt-grt-pl-qtz ± sil
	bt-sil-crd-grt-kfs-pl-qtz	crd-grt-sil-kfs-pl-gtz ± bt ± hc	bt-crd-grt-qtz ± ged
	crd-hc-sil-qtz	crd-grt-opx-bt-pl-qtz	bt-opx-pl-qtz
	grt-opx-pl-qtz		
		opx-pl-qtz ± grt	ged-grt-qtz ± pl
		opx-crd-qtz ± grt ± ged	grt-opx-pl-qtz
		opx-grt-qtz	grt-pl-qtz
		grt-pl-qtz	crd-grt-ged-qtz ± pl ± bt
			crd-ged-qtz ± pl ± bt
Block V, Korppinen	Block VI, Pihtipudas		grt-cum-pl-qtz
bt-grt-pl-qtz	bt-ms-and-pl-qtz ± grt		opx-crd-qtz
bt-sil-pl-qtz ± grt	bt-ms-crd-pl-qtz		ged-pl-qtz
bt-ged-pl-qtz ± grt	bt-ms-grt-pl-qtz ± tur		
bt-crd-pl-qtz	bt-grt-st-pl-qtz ± ms		
bt-ms-pl-qtz	bt-st-and-qtz ± ms		
bt-pl-kfs-qtz			
bt-crd-grt-sil-kfs-qtz-hc			
bt-crd-grt-st-sil-hc-pl-qtz			

Table 2. Reactions in peraluminous rocks after the temperature maximum.

Block I, Vieremä	Block II, Lampaanjärvi	Block III, Pielavesi	Block IV, Osmanki
st + bt + V = ms + chl	kfs + sil + V = ms + qtz	opx + pl = grt + qtz	crd + kfs + V = bt + sil + qtz
	sil + qtz + V + K^+ = ms	opx + crd = grt + qtz	grt + gtz + V = ged + crd
	crd + kfs + V = bt + and/sil + qtz	opx + ts = grt	opx + qtz + V = ath
	grt + qtz + V + K^+ = bt + ms	hc + qtz = crd	opx + qtz + V = cum
	grt + kfs + V = bt + ms + and/sil + qtz	grt = crd + sil + qtz	ged + V = chl + qtz
		crd + kfs + V = bt + sil/and + qtz	
		crd + sil + V = st + qtz	
		opx + qtz + V = ath/cum	
		opx + kfs/K^+ + V = bt + qtz	
		crd = opx + sil + qtz + V	
		pl = grt + sil + qtz	
		pl + Fe-ox + qtz = grt	
Block V, Korppinen	**Block VI, Pihtipudas**		
grt + bt + V = chl + ms + qtz	and + bt + V = chl + ms		
crd + bt + V = chl + ms + qtz	and + qtz + V + K^2 = ms		
crd + sil + V = st + qtz			
crd + kfs + V = bt + ms + qtz			

tion phase, which corresponds to the D_b of Pajunen, is seen as ductile and brittle faulting trending northeast and northwest. Associated with it, the porphyritic granites and mangerites were emplaced. Rigid north-south trending faulting uplifted the eastern part of the area in relation to the western one.

According to deep-seismic sounding, SVEKA, (Luosto *et al.*, 1984; Grad and Luosto, 1987) the crust has deep shears and tectonic disturbances that extend to the mantle. Korsman *et al.* (1984) demonstrated that they are visible on the erosion surface as faults at which the metamorphic grade changes. The Kinturi shear line, which trends northwest-southeast, and was attributed by Ward to D_3 and by Pajunen to D_b, shows up in the SVEKA profile as a deep shear extending to Moho. Associated with it in the Pielavesi—Pihtipudas area there is a change in metamorphic grade on the erosion surface. According to Grad and Luosto (1987), the average crustal thickness in the Baltic Shield is about 45 km. In the central part of the SVEKA profile (the Ladoga — Bothnian Bay zone), the average crustal thickness is 56 km, the maximum being 59 km. On the erosion surface the maximum thickening is approximately at blocks III—V.

Block I, Vieremä

The metapelites of the Vieremä block have staurolite-bearing horizons with large staurolite porphyroblasts up to several centimetres long. In the north of the zone, fibrous sillimanite has been encountered, and in the south, there are mica schists that contain fine-grained garnets. Retrograde hydration reactions were fairly intense, altering the margins of the staurolite grains into chlorite and muscovite. In places alteration was total, resulting in the formation of euhedral pseudomorphs filled with chlorite and muscovite. At the same time, abundant chlorite crystallized in the matrix. The biotite around the staurolite grains was consumed in the course of the reaction.

Block II, Lampaanjärvi

Staurolite is no longer encountered in the Lampaanjärvi block except as small relict inclusions in pseudomorphs filled with muscovite, sillimanite and biotite. Sillimanite occurs as both coarse and fibrous grains. Near the mangerite intrusions cordierite appears in the metapelites at the same time as some muscovite disappears (Fig. 1). With a further increase in metamorphic grade, the assemblage bt-sil-crd-kfs-pl-qtz becomes equilibrated followed by the assemblage bt-sil-grt-crd-kfs-pl-qtz. Melting started at the same time, resulting in the formation of granitic veins and portions in metapelites that account for 10—15 % of the volume of the rock. The mineralogical changes, from the appearance of cordierite to the equilibration of garnet and cordierite, took place within a zone 1—3 km wide.

The mafic volcanics in the garnet-cordierite zone contain hypersthene in the vicinity of intrusions, in addition to which the cordierite in the metagreywackes often has spinel inclusions.

The mangerite intrusions are surrounded by contact aureoles about 100—200 m wide in which the rocks are in places migmatitic and the abundances of garnet and potassium feldspar increase while those of biotite and sillimanite decrease relative to those in the environment.

In the contact aureoles large garnet grains, which are rich in quartz inclusions and more than 1 cm in diameter, are surrounded by migmatizing granite (Fig. 3b). This is an indication of the dehydration melting of biotite, in which garnet, potassium feldspar and melt (Thompson, 1982) were formed locally as a result of a reaction between biotite, sillimanite and quartz. Assemblages of grt-opx-pl-qtz and opx-bt-kfs-qtz are in equilibrium right at the contact with the mangerites and in the metapelite xenoliths within the mangerites.

The cordierite in the vicinity of the contact (less than 100 m) of the Vaaraslahti mangerite (Fig. 2) shows sector trilling.

When the temperature rose as a result of the thermal effect of the mangerites the following reactions took place in the metapelites

(1) ms + qtz = kfs + sil + H_2O (isograd muscovite out, Fig. 1)
(2) bt + sil + qtz = crd + kfs + H_2O (isograd crd-kfs-bt-sil-qtz in, Fig. 1)
(3) bt + sil + qtz = grt + crd + kfs + H_2O (isograd grt-crd-kfs-bt-sil-qtz in, Fig. 1)
(4) crd = hc + qtz + H_2O
(5) crd = grt + sil + qtz + H_2O
(6) bt + sil + qtz = grt + kfs + H_2O
(7) bt + sil + qtz = grt + kfs + liquid
(8) pl + opx = grt + qtz
(9) bt + qtz = opx + kfs + H_2O

Reaction 7 is visible in the 100—200 m wide contact aureole (Fig. 3b), reactions 8—9 were observed in Vaaraslahti from metapelites in the innermost aureole only a few metres from the contact. Reaction (4) is problematic as spinel occurs only as inclusions in cordierite but never in contact with quartz. It is possible that the reaction advanced later from right to left, resulting in the disappearance of quartz adjacent to hercynite.

Retrograde metamorphism affected the whole block very strongly. Sillimanite and potassium feldspar were altered to muscovite, garnet turned to biotite and muscovite, and cordierite and garnet were often altered to greenish biotite, sillimanite and andalusite. Cordierite grains filled with biotite, fibrous sillimanite, andalusite and quartz are typical features. Andalusite is fine-grained and occurs either as symplectic intergrowths with cordierite (cf. Korsman *et al.*, 1984) or together with biotite. The retrograde alteration of cordierite to andalusite and biotite is also visible in the contact aureoles of the mangerites; the reaction was thus postmagmatic. The alterations that produced muscovite and biotite as a result of decomposition of sillimanite and cordierite are common in the potassium-deficient rocks, too. This implies that either potassium feldspar was totally consumed in the reactions or that the reactions took place with a potassium-

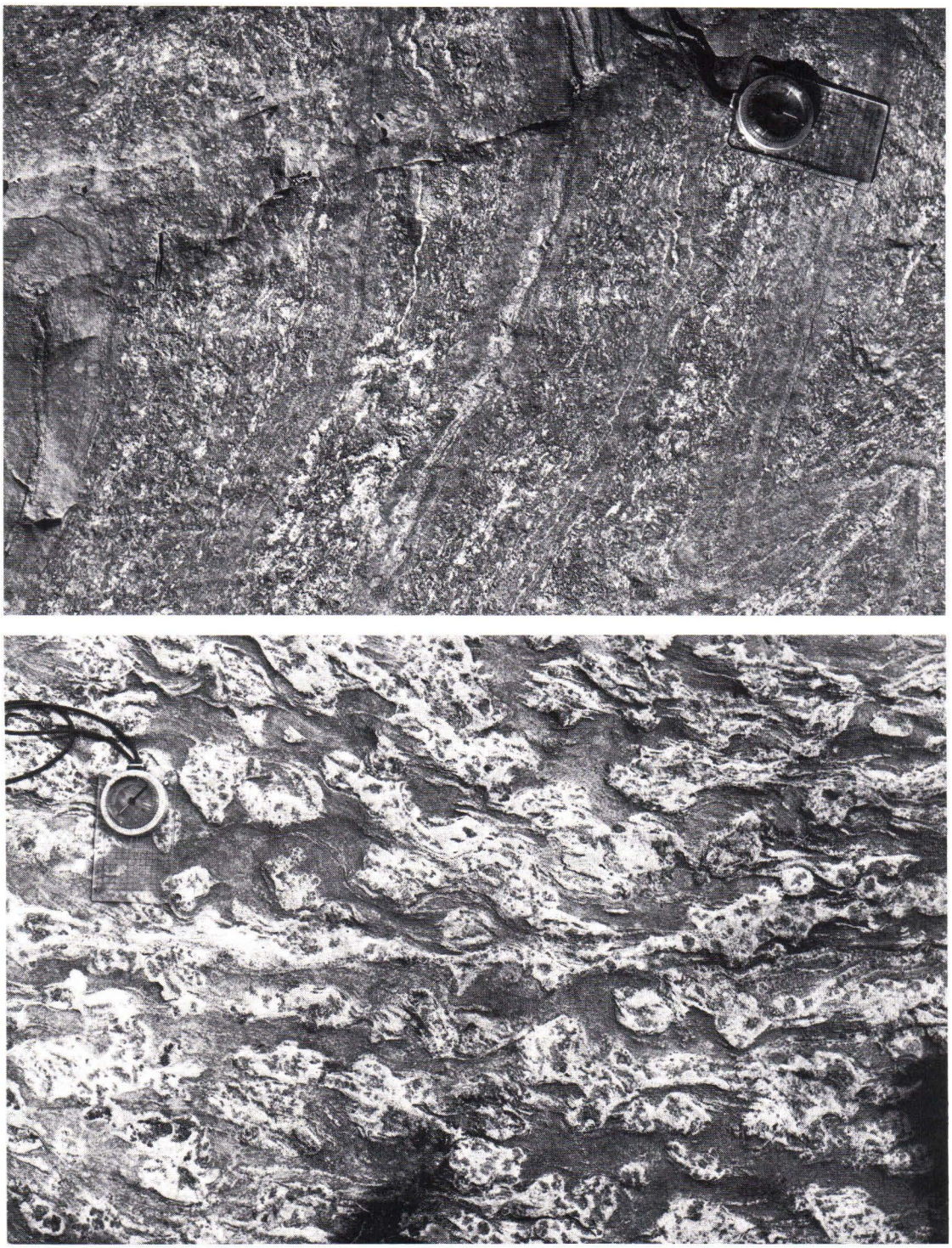

Fig. 3. Metagreywacke of the Lampaanjärvi block (II), a) from outcrop 36 (Fig. 2) about 2 km from the nearest mangerite intrusion, and b) from outcrop 48, about 30 m from the contact of the Vaaraslahti mangerite intrusion.

bearing fluid. The paragonite component is low in all the muscovites analysed (Table 3, location of the samples is shown in Fig. 2; map coordinates in appendix), suggesting that the retrograde muscovitization of sillimanite, with plagioclase as reactant, was of minor importance.

Table 3. Muscovite analyses. Analysis 3 refers to muscovite altered from garnet.

Code	1	2	3	4	5	6	7
Block	I	II	II	V	V	VI	VI
SiO_2	46.07	46.72	46.47	46.08	46.10	45.87	45.89
TiO_2	0.34	0.40	0.09	0.44	0.29	0.31	0.56
Al_2O_3	35.71	35.22	34.52	34.24	33.86	34.28	34.31
FeO	0.95	0.97	1.07	2.33	2.73	1.54	1.60
MnO	0.01	0.03	0.00	0.00	0.01	0.03	0.00
MgO	0.42	0.61	0.72	0.56	0.67	0.52	0.46
CaO	0.00	0.02	0.00	0.01	0.00	0.00	0.03
Na_2O	1.18	0.76	0.78	1.02	0.90	0.97	0.98
K_2O	8.81	9.16	9.68	8.98	9.32	9.15	8.66
V_2O_3	0.05	0.05	0.02	0.03	0.01	0.05	0.07
CR_2O_3	0.03	0.03	0.00	0.00	0.01	0.03	0.03
NiO	0.00	0.00	0.00	0.00	0.01	0.00	0.00
Total	93.56	93.96	93.36	93.69	93.91	92.77	92.58
Number of cations based on 22 oxygens							
Si	6.1781	6.2394	6.2710	6.2225	6.2357	6.2375	6.2353
Ti	0.0346	0.0399	0.0086	0.0447	0.0292	0.0321	0.0568
Al	5.6432	5.5441	5.4901	5.4504	5.3979	5.4936	5.4939
Fe	0.1068	0.1079	0.1206	0.2634	0.3093	0.1752	0.1817
Mn	0.0009	0.0029	0.0006	0.0000	0.0009	0.0035	0.0000
Mg	0.0835	0.1212	0.1456	0.1133	0.1357	0.1058	0.0934
Ca	0.0001	0.0024	0.0000	0.0009	0.0007	0.0001	0.0039
K	1.5065	1.5603	1.6663	1.5467	1.6081	1.5875	1.5018
Na	0.3065	0.1960	0.2038	0.2666	0.2363	0.2568	0.2577
V_2O_3	0.0054	0.0048	0.0025	0.0037	0.0012	0.0056	0.0075
Cr_2O_3	0.0027	0.0035	0.0000	0.0000	0.0007	0.0034	0.0033
NiO	0.0000	0.0002	0.0000	0.0003	0.0015	0.0000	0.0000

Block III, Pielavesi

A more detailed description of the PT evolution of the Pielavesi block will be given later; the present section deals only with general features. The mica gneisses in the block are predominantly nebulitic migmatites without distinct neosome or palaeosome, although veined gneisses are also encountered.

Most of the mica gneisses contain abundant biotite, as the excess of aluminium over alkalis and calcium is not great; sillimanite is rather rare, implying that the decomposition of biotite did not advance far.

The garnet-cordierite-hypersthene rocks are coarse-grained, with abundant garnet and hypersthene grains 1—2 cm in diameter.

The dioritic-tonalitic rocks and the amphibolites have the assemblage hbl-opx-pl-qtz ± cpx ± bt.

Block IV, Osmanki

The zone of high metamorphic grade continues northwards into the Osmanki block from the Pielavesi block as transitional granulites, with the difference that the two-pyroxene assemblages disappear from the tonalitic-dioritic rocks, and the grt-crd-opx assemblage is replaced by the grt-crd-oam assemblage in the rocks of corresponding composition. Orthopyroxene is an occasional constituent in the grt-crd-oam rocks and in amphibolites.

In places staurolite occurs as small relict inclusions in cordierite. In the sillimanite-bearing rocks, a cordierite rim has often developed around garnet grains. Cordierite has undergone retrograde alteration into biotite and Al silicate, which is predominantly fine-grained or fibrous sillimanite. In general, the reaction has not advanced as far as in the Lampaanjärvi block.

Orthopyroxene has almost invariably altered to cummingtonite or anthophyllite and the latter further to chlorite. The garnet-cordierite-orthoamphibole rocks frequently show complex crystallization textures (Hudson & Hölttä, in prep.). Hence, garnet, for example, has altered to cordierite-orthoamphibole symplectites along the margins, and staurolite and spinel are rimmed by cordierite when surrounded by orthoamphibole.

Block V, Korppinen

Garnet-cordierite equilibrium is rare in the Korppinen block; it appears that the maximum temperature conditions in the block were between those of the muscovite decomposition reaction and the garnet-cordierite equilibrium. The assemblage grt-crd-st-bt-sil-spl-pl-qtz has been encountered in a mica schist xenolith embedded in a gabbro in the southern part of the zone. The magnesium contents of garnet and cordierite in this assemblage are fairly high in relation to the environment (Table 5, sample no. 44), suggesting that the xenolith might have been transported from considerable depths by the intruding magma. Muscovite and chlorite are common retrograde phases, particularly in the numerous shear zones in the area. The mica gneisses adjacent to the Pyhäsalmi ore deposit, which is located about 2 km southeast of Pyhäjärvi village (Fig. 1), contain abundant muscovite in the assemblages ms-bt-qtz and crd-phl-ms-qtz, which, however, may be due to late hydrothermal activity associated with the emplacement of the ore (cf. Pajunen, 1988). Potassium feldspar is a rare constituent in the metagreywackes, probably partly because of intense biotitization and muscovitization during retrograde metamorphism.

The small staurolite inclusions often present in the cordierite grains or pseudomorphs are prograde relics. The retrograde alteration of cordierite has often resulted in the formation of sillimanite, although andalusite is also encountered as a rare constituent. Plagioclase and cordierite rims have grown around garnet in sillimanite-bearing rocks.

Block VI, Pihtipudas

Pelitic rocks are rather rare in the Pihtipudas block. Narrow metagreywacke horizons have been encountered in the village of Pihtipudas, at Virkamäki and Haasiapuro west of the lake Pyhäjärvi. They often contain andalusite as large grains measuring about one centimetre.

Sillimanite is rare and has only been met with as acicular crystals at the margin of andalusite

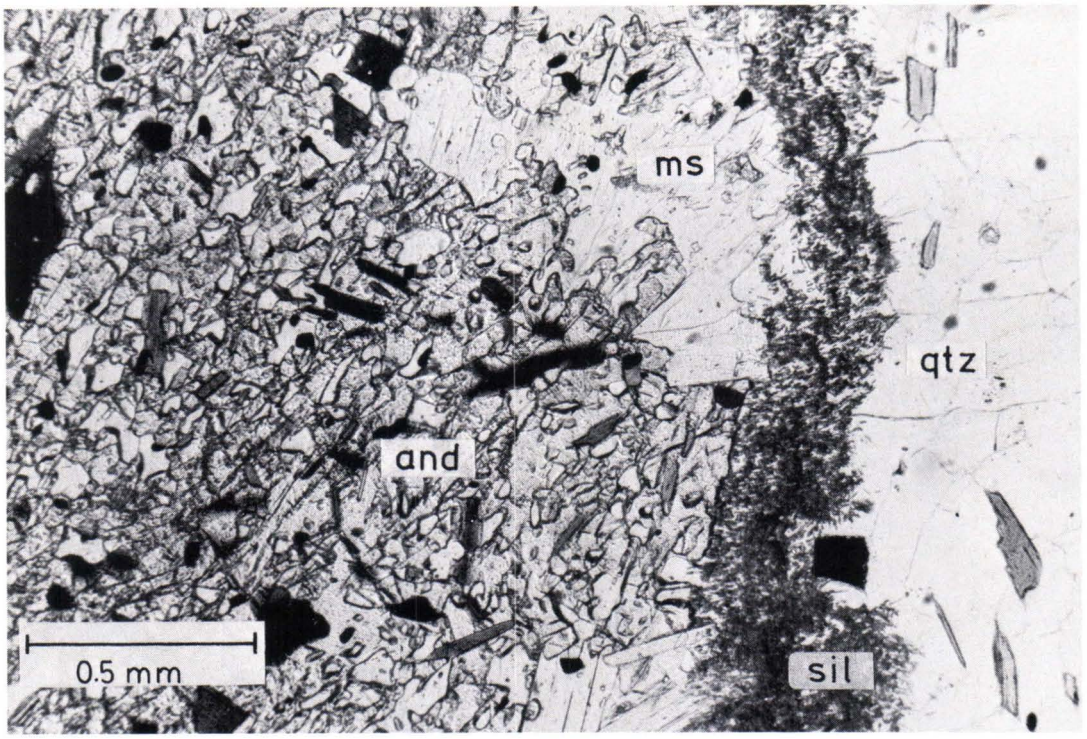

Fig. 4. Acicular sillimanite crystallized on an andalusite grain. Outcrop 7 in Fig. 2.

(Fig. 4). The alteration took place both directly and via muscovite. Chlorite is a retrograde phase, as is obviously some of the muscovite. During the prograde stage staurolite was partly decomposed in the metapelites through the reaction

(10) st + ms + qtz = and + bt + grt + H_2O

In places garnet crystallized close to andalusite, probably through the reaction:

(11) bt + and + qtz = grt + ms

Staurolite has altered to chlorite and muscovite along the margins, as at Vieremä (Table 2). In places andalusite has been decomposed by the reactions

(12) and + bt + H_2O = chl + ms

(13) and + qtz + H_2O + K^+ = ms

The occurrence of reaction (13) is supported by the absence of potassium feldspar from metagreywackes.

PT DETERMINATIONS

Chemical data for minerals

The majority of the electron probe microanalyses were made at the Institute of Electron Optics, University of Oulu, using a JEOL JCXA — 733 microprobe.

The acceleration voltage was 15 kV, the current of the electron beam 30 nA and the beam diameter 10 μm. The standards used were cleavelandite (Na), periclase (Mg), synth. sapphire (Al), quartz (Si), sanidine (K), wollastonite (Ca), synth. TiO (Ti), haematite (Fe) and correspond-

ing metals (V, Cr, Mn, Zn). Some of the analyses were made at the Geological Survey of Finland, Espoo, with a JEOL JCXA — 733 microprobe. The acceleration voltage and the beam diameter were the same as in Oulu; the current of the electron beam was 25 nA. The standards used at the GSF were albite (Si, Na), rutile (Ti), almandine (Fe), rhodonite (Mn), diopside (Mg, Ca), sanidine (K) and synth. yttrium aluminium garnet (Al).

V, Cr, Ni and Zn were not analysed with the GSF probe. Most of the analyses presented in Tables 3 and 9—16 represent one analysis per point. Some of the analyses were repeated and the deviation in oxide weight per centages was normally only a few tenths. ZAF correction programs were used.

Thermobarometry

The crystallization temperature was determined using garnet-biotite, garnet-cordierite and garnet-orthopyroxene thermometers. Since the composition of the margins of the garnet grains was altered by intense retrograde metamorphism, the tabulated data refer to the composition of the garnet cores unless specially mentioned. The highest Mg contents in garnet in blocks II—V were recorded from the cores of the largest garnet grains, which can be considered to represent equilibration close to the maximum temperature. Small garnets that crystallized during cooling or represent blocking (Thompson and England, 1984) or the margins of the large grains in thin sections contain markedly less magnesium and therefore give lower crystallization temperatures.

Since biotite readily undergoes retrograde re-equilibration, minerals that were not in direct contact with garnet were chosen for the computations. Table 4 lists the temperatures given by garnet-biotite thermometers, calculated as proposed by Ferry and Spear (1978), Ganguly and Saxena (1984), Pigage and Greenwood (1982), Perchuk and Lavrenteva (1983), Indares and Martignole (1985) and Hodges and Spear (1982). Factors affecting the results given by the thermometers have been discussed in many papers (e.g. Hudson, 1985; Tuisku and Sivonen, 1984). In their experimental studies, Ferry and Spear, and Perchuk and Lavrenteva considered garnets ideal Fe-Mg mixtures. Hodges and Spear formulated the thermometry of Ferry and Spear by considering garnet as a nonideal symmetric four-component mixture according to Ganguly and Kennedy (1974); the mixing model of Ganguly and Saxena (op. cit.) assumes asymmetric enthalpy and symmetric entropy of mixing. The results calculated using the procedure of Hodges and Spear are no more than 20°C higher than those given by the procedure of Ferry and Spear, except for the highest spessartite and grossularite contents, for which the results given by the latter thermometry are clearly too low for the assemblages.

The garnet-cordierite temperatures calculated with the procedure of Holdaway and Lee (1977) are given in Table 6. In the Pielavesi block temperatures are mostly lower than those given by the other thermometers, even in the case of the highest pyrope contents. This is in harmony with the observations on the granulites of Enderby Land made by Ellis (1980) and Harley (1986), who concluded that not enough is known about the equilibration of garnet and cordierite and about Fe-Mg cation exchange at high temperatures. The high Mg content in cordierite due to fairly high pressure affects the thermometry by keeping the temperatures too low when the pressure increases. When in contact with garnet, cordierite, like biotite, is richer in Mg than is the matrix cordierite. The highest temperature that the garnet-cordierite thermometer showed for the Pielavesi block, c. 780°C, was obtained from the composition of the core of a large garnet grain and cordierite that was not in direct contact with the garnet.

Table 4. Garnet-biotite temperatures. F&S = Ferry & Spear 1978, G&S = Ganguly&Saxena 1984, P&G = Pigage & Greenwood 1982, P&L = Perchuk & Lavrenteva 1983, H&S = Hodges & Spear 1982, IM_1 = equation 18, IM_2 = equation 19 according to Indares & Martignole 1985. In block II, the number following the code refers to the distance from the contact of the Vaaraslahti mangerite intrusion. In block III, 21-ig refers to the retrograde grt-bt intergrowth (as in Fig. 12). The letter r after the code indicates that the calculations were based on the composition of the garnet rim. The letter combination -r-i refers to the garnet rim and plus biotite inclusion (see Fig. 6).

Code	X_{Fe}Grt	X_{Mn}Grt	X_{Mg}Grt	X_{Ca}Grt	X_{Fe}Bt	X_{Mg}Bt	X_{Al}viBt	X_{Ti}Bt	F&S	G&S	P&G	P&L	H&S	IM_1	IM_2
Block I.															
1	0.722	0.126	0.113	0.039	0.377	0.386	0.212	0.024	528	542	613	544	543	495	524
1a	0.742	0.114	0.112	0.032	0.423	0.367	0.177	0.031	568	580	647	569	580	523	553
1b-r	0.755	0.106	0.103	0.036	0.446	0.395	0.130	0.026	526	544	600	552	540	495	530
1b	0.709	0.145	0.104	0.042	0.446	0.395	0.130	0.026	552	577	651	553	569	522	583
Block II.															
2	0.681	0.145	0.130	0.045	0.422	0.384	0.155	0.035	635	643	745	589	653	588	648
8	0.709	0.028	0.198	0.065	0.343	0.509	0.125	0.023	596	535	653	599	623	579	578
9	0.764	0.053	0.150	0.034	0.409	0.405	0.130	0.056	616	588	667	600	630	538	540
10	0.734	0.022	0.220	0.024	0.364	0.415	0.145	0.075	736	635	768	666	746	609	581
11—400m.	0.752	0.026	0.186	0.036	0.433	0.376	0.107	0.083	776	704	821	683	791	641	628
12—450m.	0.749	0.026	0.197	0.028	0.394	0.424	0.119	0.061	702	624	738	649	714	606	591
13—150m.	0.693	0.039	0.224	0.044	0.385	0.442	0.112	0.060	771	674	830	676	789	677	679
14—80m.	0.728	0.025	0.216	0.031	0.392	0.437	0.101	0.071	742	646	781	668	755	629	618
38—2m.	0.764	0.018	0.193	0.024	0.385	0.466	0.072	0.076	638	565	664	619	648	531	519
Block III.															
15	0.643	0.025	0.300	0.032	0.371	0.502	0.026	0.100	889	715	934	721	902	715	722
16	0.602	0.105	0.263	0.030	0.303	0.514	0.139	0.044	732	632	818	628	745	659	697
17	0.695	0.015	0.264	0.027	0.320	0.503	0.121	0.103	697	568	725	649	708	532	515
18	0.628	0.014	0.329	0.030	0.328	0.515	0.096	0.061	868	674	903	717	881	759	741
19	0.586	0.012	0.367	0.035	0.307	0.544	0.059	0.090	906	686	945	732	921	745	734
20	0.660	0.007	0.303	0.029	0.318	0.546	0.064	0.071	748	586	775	667	760	638	623
21-ig	0.696	0.017	0.267	0.019	0.251	0.626	0.080	0.043	536	426	556	556	544	482	472
39a	0.667	0.019	0.286	0.028	0.313	0.507	0.117	0.063	737	591	770	667	749	635	615
39a-r-i	0.695	0.022	0.251	0.032	0.213	0.602	0.143	0.042	473	382	501	541	485	423	406
Block IV.															
22	0.696	0.034	0.246	0.024	0.390	0.500	0.078	0.031	760	641	800	673	770	711	716
23	0.686	0.009	0.267	0.038	0.319	0.499	0.108	0.073	710	579	743	658	726	599	576
Block V.															
25	0.681	0.055	0.254	0.010	0.359	0.497	0.109	0.034	747	626	788	660	751	683	691
26	0.733	0.065	0.087	0.115	0.474	0.301	0.183	0.041	598	637	706	587	643	568	585
27	0.742	0.062	0.183	0.014	0.394	0.418	0.165	0.023	680	621	726	629	686	634	634
28	0.774	0.059	0.157	0.010	0.381	0.382	0.222	0.014	625	587	664	603	629	587	571

29	0.673	0.110	0.165	0.052	0.372	0.463	0.133	0.030	615	592	709	583	636	581	626
30	0.692	0.063	0.179	0.067	0.400	0.432	0.134	0.032	693	649	778	634	720	657	678
31	0.717	0.059	0.199	0.024	0.381	0.442	0.158	0.016	694	623	747	636	704	664	667
Block VI.															
32	0.433	0.364	0.057	0.145	0.383	0.428	0.161	0.023	449	550	691	451	503	464	639
32a	0.412	0.377	0.062	0.149	0.425	0.407	0.131	0.033	528	641	805	484	585	532	743
32a-r	0.610	0.203	0.091	0.096	0.425	0.407	0.131	0.033	524	577	682	537	562	508	609
32b-r	0.592	0.219	0.116	0.073	0.373	0.423	0.174	0.026	557	595	716	550	586	535	637
7	0.718	0.158	0.085	0.039	0.489	0.311	0.158	0.038	584	627	693	583	599	532	595
6	0.714	0.168	0.077	0.042	0.479	0.315	0.162	0.040	541	590	651	558	557	490	554

Table 5. Pressures calculated from the garnet-plagioclase-biotite-muscovite barometer. P_1 = P-Mg, P_2 = P-Fe according to Ghent & Stout (1981), P_3 = according to Hodges & Crowley (1985).

Code	T(°C)	$X_{Ca}Pl$	$X_{Mg}Bt$	$X_{Fe}Bt$	$X_{K}Ms$	$X_{Al}viMs$	$X_{Na}Ms$	$X_{Fe}Grt$	$X_{Mn}Grt$	$X_{Mg}Grt$	$X_{Ca}Grt$	P_1	P_2	P_3
Block I														
1c	580	0.233	0.395	0.446	0.831	0.944	0.169	0.709	0.145	0.104	0.042	4.1	4.4	4.8
1d	580	0.224	0.367	0.423	0.810	0.940	0.190	0.742	0.114	0.112	0.032	3.8	3.9	4.4
Block II														
2a	650	0.289	0.384	0.422	0.887	0.932	0.112	0.681	0.145	0.129	0.045	4.3	4.5	5.8
3	650	0.172	0.371	0.457	0.891	0.932	0.109	0.833	0.054	0.092	0.021	2.6	4.1	5.2
Block VI														
6	600	0.338	0.315	0.479	0.861	0.922	0.139	0.713	0.168	0.077	0.042	2.7	3.2	3.8
7	600	0.328	0.311	0.489	0.851	0.917	0.146	0.718	0.158	0.085	0.039	2.9	3.0	3.6
32c	600	0.352	0.428	0.383	0.829	0.891	0.171	0.433	0.364	0.057	0.145	4.4	5.8	6.3

Table 6. Garnet-cordierite temperatures and pressures calculated according to Holdaway and Lee (1977). An asterisk after the pressure value implies that sillimanite is absent from the assemblage and that the pressures are thus maximum pressures. In block II, the last number of the sample code refers to the distance from the contact of the Vaaraslahti mangerite intrusion (Fig. 2). Calculations based on the partial pressure of water of 0.4.

Code	$X_{Fe}Grt$	$X_{Mn}Grt$	$X_{Mg}Grt$	$X_{Ca}Grt$	$X_{Mg}Crd$	P(kb)	T°C
Block II.							
33	0.740	0.013	0.215	0.030	0.736	6.0	606
34	0.749	0.017	0.203	0.029	0.678	5.3	663
35	0.742	0.020	0.212	0.025	0.684	5.4	668
36	0.763	0.031	0.172	0.031	0.697	5.6	592
12—450m.	0.748	0.026	0.196	0.028	0.659	5.2	677
14—80m.	0.728	0.025	0.215	0.030	0.665	5.1	704
37—20m.	0.724	0.015	0.226	0.032	0.648	4.9	746
38—2m.	0.763	0.018	0.193	0.024	0.594	4.5	752
Block III.							
20	0.660	0.007	0.303	0.028	0.786	6.2	652
19	0.586	0.012	0.367	0.035	0.782	5.8	755
19b	0.677	0.010	0.287	0.023	0.785	6.3	631
19a	0.627	0.011	0.329	0.032	0.787	6.1	689
21a	0.650	0.025	0.300	0.023	0.722	5.3*	761
39	0.691	0.028	0.249	0.030	0.758	6.0	631
40	0.564	0.104	0.318	0.014	0.736	5.2	782
Block IV.							
24a	0.682	0.011	0.271	0.035	0.742	5.8	680
22	0.672	0.031	0.276	0.020	0.730	5.6	706
23a	0.677	0.008	0.274	0.039	0.759	5.9	660
41	0.594	0.008	0.360	0.036	0.798	6.1	708
42	0.684	0.006	0.279	0.029	0.729	5.6*	709
Block V.							
31	0.717	0.058	0.199	0.024	0.643	5.0	702
31a	0.761	0.063	0.169	0.005	0.643	5.2	640
27	0.741	0.061	0.182	0.013	0.626	4.9	695
43	0.673	0.025	0.266	0.035	0.743	5.7*	675
44	0.659	0.004	0.321	0.014	0.812	6.6	626

The garnet-orthopyroxene thermometer was used to study PT evolution in the Pielavesi granulite block. The temperature was calculated with the aid of the calibrations of Harley (1984a), Sen and Bhattacharya (1984) and Perchuk *et al.* (1985). The calibration of Sen and Bhattacharya gave higher temperatures than the other two thermometers. The maximum temperatures derived from the calibrations of Harley and Perchuk *et al.* were also fairly high. However, they correspond to the maximum temperatures reported from other Precambrian granulite areas (e.g. Ellis & Green, 1985; Jansen *et al.*, 1985). The higher temperatures were obtained from the compositions of the cores of grains with a diameter of up to one centimetre. Minerals formed by the reactions under declining temperature conditions gave lower temperatures, and the lowest temperature, c. 600°C, was recorded when the calculations were based on the composition of the outermost diffusion rim. The temperatures deduced from the garnet-orthopyroxene pair are listed in Table 17.

Pressure was determined with the aid of geobarometers based on the garnet-plagioclase-sillimanite-quartz (Newton & Haselton, 1981, Table 7), garnet-cordierite-sillimanite-quartz (Holdaway & Lee, 1977, Table 6), garnet-

Table 7. Garnet-plagioclase pressures calculated according to Newton & Haselton (1981) with the following changes: P°(sil) = —1.17 + 0.238T(°C) (Ganguly & Saxena 1984, p. 93); P°(and) = —1.99 + 0.028T(°C) (St-Onge 1984, p. 204, andalusite is the stable Al silicate in block VI). In block II, the number after the code refers to the distance in metres from the contact of the Vaaraslahti mangerite intrusion. The letter combination -r-c denotes that the calculations were based on the composition of the garnet rim end of the enveloping plagioclase corona. The letter r refers to the garnet rim and the letter i indicates that the calculations were based on the plagioclase inclusion in garnet.

Code	T(°C)	$X_{Ca}Pl$	$X_{Fe}Grt$	$X_{Mn}Grt$	$X_{Mg}Grt$	$X_{Ca}Grt$	P(kb)
Block II.							
45	650	0.317	0.739	0.025	0.203	0.033	3.6
2a	650	0.290	0.681	0.145	0.130	0.045	4.8
3a	650	0.172	0.787	0.028	0.166	0.019	4.2
3b	650	0.220	0.764	0.038	0.170	0.028	4.5
46	680	0.306	0.775	0.051	0.143	0.032	3.8
36a	680	0.297	0.777	0.037	0.150	0.037	4.6
9	650	0.288	0.764	0.053	0.150	0.034	3.9
47—300m.	680	0.303	0.746	0.032	0.184	0.037	4.6
47—300m-r-c	680	0.293	0.756	0.032	0.179	0.032	4.2
13a—150m.	680	0.272	0.757	0.025	0.186	0.032	4.5
14a—80m.	700	0.294	0.738	0.036	0.182	0.044	5.8
37—20m.	750	0.277	0.725	0.016	0.227	0.032	5.8
38a—2m.	750	0.264	0.771	0.020	0.185	0.025	4.7
48—2m.	750	0.256	0.699	0.013	0.262	0.025	5.3
Block III.							
19	800	0.344	0.586	0.012	0.367	0.035	6.4
49-i	800	0.806	0.658	0.025	0.263	0.054	5.5
50-i	800	0.375	0.612	0.086	0.265	0.037	5.8
39a	800	0.275	0.657	0.020	0.287	0.036	7.5
39a-r	600	0.303	0.701	0.028	0.238	0.033	3.1
39a-i	800	0.563	0.657	0.020	0.287	0.036	4.5
Block IV.							
24a	750	0.297	0.683	0.011	0.297	0.035	6.0
23	750	0.343	0.686	0.009	0.267	0.038	5.7
41	700	0.291	0.594	0.009	0.360	0.036	5.8
41a-i	700	0.081	0.730	0.010	0.232	0.028	11.2
Block V.							
51	680	0.341	0.755	0.009	0.198	0.039	4.4
51a-r-c	680	0.241	0.752	0.010	0.201	0.036	5.7
28a	680	0.128	0.753	0.059	0.173	0.016	5.5
28	680	0.080	0.774	0.059	0.157	0.010	6.1
26	650	0.409	0.733	0.065	0.087	0.115	7.6
26a	650	0.435	0.813	0.033	0.108	0.045	3.4
25	700	0.201	0.681	0.055	0.254	0.010	1.9
30-i	650	0.416	0.692	0.063	0.179	0.067	5.4
30a	650	0.429	0.695	0.065	0.175	0.064	5.1
30a-r-c	650	0.452	0.713	0.084	0.143	0.060	4.6
31b	700	0.270	0.710	0.077	0.180	0.033	5.0
Block VI.							
32b-r	600	0.427	0.592	0.219	0.116	0.073	5.8
6	600	0.338	0.714	0.168	0.077	0.042	3.9
7	600	0.328	0.718	0.158	0.085	0.039	3.8

plagioclase-biotite-muscovite (Ghent and Stout, 1981; Hodges and Crowley, 1985, Table 5) and garnet-orthopyroxene-plagioclase-quartz assemblages (Newton & Perkins, 1982; Perkins &

Chipera, 1985, Table 17).

On account of temperature dependence, the maximum temperatures given by the thermometers for each zone were used when computing pressures for the grt-pl-Al-sil-qtz and grt-bt-pl-mu barometers. The grt-crd-sil-qtz and grt-opx-pl-qtz barometers are not so much temperature-dependent, and hence the thermometer and barometer equations were solved simultaneously.

No aluminium silicate was found in the garnetiferous rocks of the Vieremä schist belt (block I), and so only the grt-pl-bt-ms barometer was used for the zone. The above barometer and the grt-pl barometer were applied to the Lampaanjärvi block (II), and the grt-crd and grt-opx-pl-qtz barometers were used for rocks showing mangerite contact effects. The garnet-plagioclase barometer (Table 7) gives a crystallization pressure that is about one kilobar lower than that given by the grt-crd barometer (Table 6) for the Lampaanjärvi block. Edwards and Essene (1988) have taken into consideration on the change in (ΔV_r) and Clapeyron slope with P and T and noticed that pressures calculated in this way are higher than those from Newton and Haselton (1981) for most metamorphic conditions. The partial water pressure has a significant effect on the results of the garnet-cordierite barometer (Holdaway & Lee 1977), and since the value of the water pressure is merely an estimate the results cannot be very accurate. Nevertheless, in the Pielavesi block the grt-crd-sil-qtz barometer indicates pressures similar to those given by the grt-opx-pl-qtz barometer at the partial water pressure of 0.4 kb (Tables 6 and 17).

The scatter in the results of the garnet-plagioclase barometer is fairly high, particularly in the Korppinen block (V), where the crystallization pressures given by the barometer vary from 1.9 to 7.6 kb when measured from the composition of the mineral cores. According to Bohlen and Lindsley (1987), the reliability range is at least ± 2 kb. This is due to the long extrapolation, the shortage of information on the reaction equilibrium of the end members and the presence of calcium that may be bound to ferric iron, all of which combine to make the activity of the grossular difficult to compute.

At Haasiapuro, in the Pihtipudas block (VI, number 32 in Tables 5 and 7), the andalusite-mica schist contains garnets that are rich in calcium. The compositions of the cores of these garnets ($X_{ca} = 0.16$) show high pressure, almost 10 kb, when the garnet-plagioclase barometer is applied. However, the calcium content declines towards the margins of the grains ($X_{ca} = 0.07$) and, considering the low metamorphic temperature, the zoning can probably be attributed to growth. Hence the grain margins are very likely in equilibrium with the rest of the assemblage. Even then the pressure is rather high, c. 6 kb, for the assemblage (grt-and-st-bt-ms-pl-qtz). The grt-pl-bt-ms barometer gives a similar pressure of (Table 5). It may be postulated that the rocks were originally metamorphosed in the kyanite field and that the present-day assemblage represents lower pressure conditions.

Shown in the PT diagram in Fig. 5 are the pressures and temperatures given by the geothermometers and geobarometers for the culmination of metamorphism in the various zones. The results are compatible with the observed mineral assemblages. The lowest P and T values, c. 3—4 kb and 550—600°C, respectively, are from block VI, where andalusite is a stable aluminium silicate. In the Vieremä schist belt (block I), where fibrous sillimanite occurs in the staurolite-mica schist, the temperature is almost the same but the pressure is slightly higher, 4—4.5 kb, in good agreement with the results of Salje (1986) for the equilibrium fields of the aluminium silicates. The crystallization pressures of the other blocks are similar, 5—6 kb, within the error limits of the barometers.

In the Lampaanjärvi block (II) the temperature rises from 620—650° to about 750°C towards the contact of the mangerites, with a simultaneous drop in pressure of about one kilobar (Tables 4, 6 and 17).

According to the thermometers and barome-

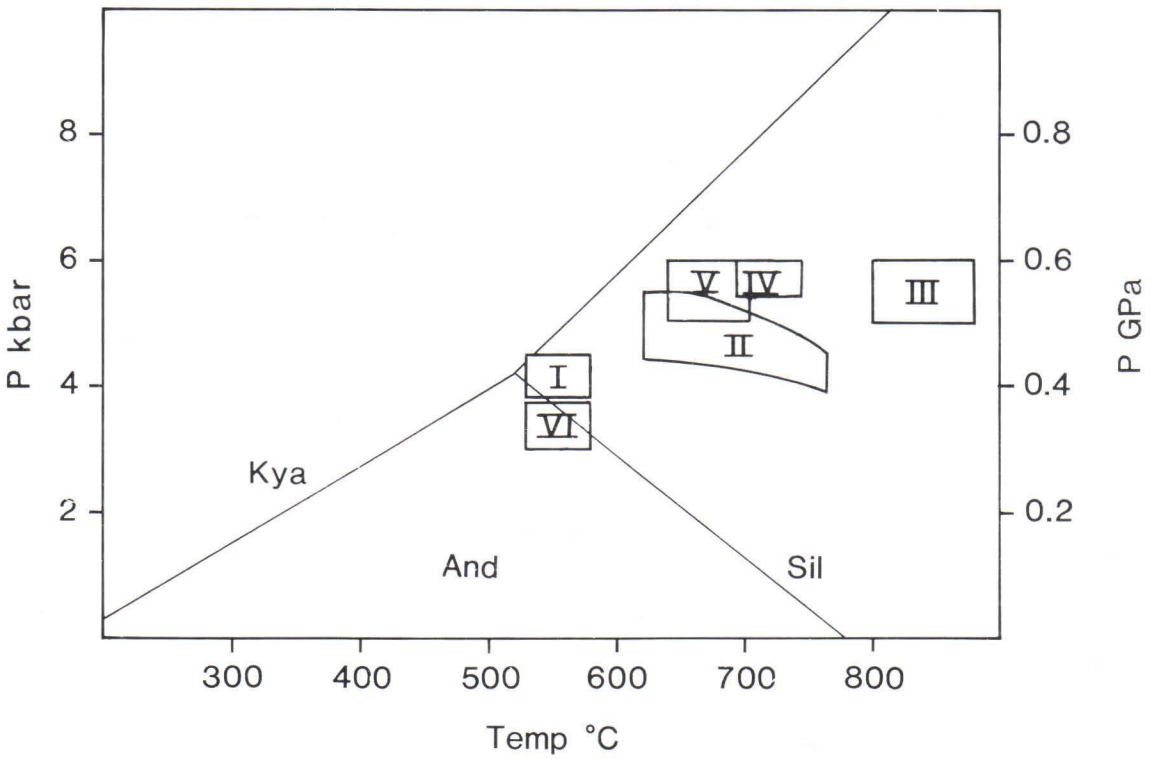

Fig. 5. PT diagram showing the temperatures and pressures at the culmination of metamorphism in the metamorphic blocks of the Pielavesi area. Blocks numbered as in Fig. 1.

ters, granulite area (III) reached a high temperature, c. 800—880°C, at a pressure of 5.5—6 kb. In block IV the temperature slightly exceeded 700°, in accord with the observed assemblages, for example, the sporadic occurrence of orthopyroxene. As shown by the thermometers, the temperature was also high in block V. The metamorphic grade may vary within a block. However, this could not be established within the scope of the present work.

The temperature path can be studied by basing the thermobarometry on the composition of the inclusions (e.g. pl, bt) in garnet (St. Onge, 1987). Poor though the garnets in the Pielavesi area are in plagioclase inclusions, it was possible to analyse plagioclase inclusions from the various blocks of the cores of a few garnet grains.

The cores of garnets grains in the granulite block (III) are often richer in Ca (Figs 6 and 17a) than the rims, or the grains have zones rich in calcium (Fig. 17a). The plagioclase inclusions in the grain core are then also richer in calcium than the matrix plagioclase (Fig. 6). If a garnet is zoned it is likely that only the inclusions are in equilibrium with the grain core. If pressure is calculated from the composition of the garnet core and matrix plagioclase the result is too high (analysis 39a, Table 7). The same probably applies to analysis 26 from block V.

Although the temperature shown by the thermometers was very high in the granulite area at the time the core of the grain crystallized, the matrix plagioclase may represent equilibrium at a lower temperature. In that case the garnet core-plagioclase inclusion and garnet rim-matrix plagioclase give almost the same pressure within the limits of error.

The plagioclase inclusion analysed from block

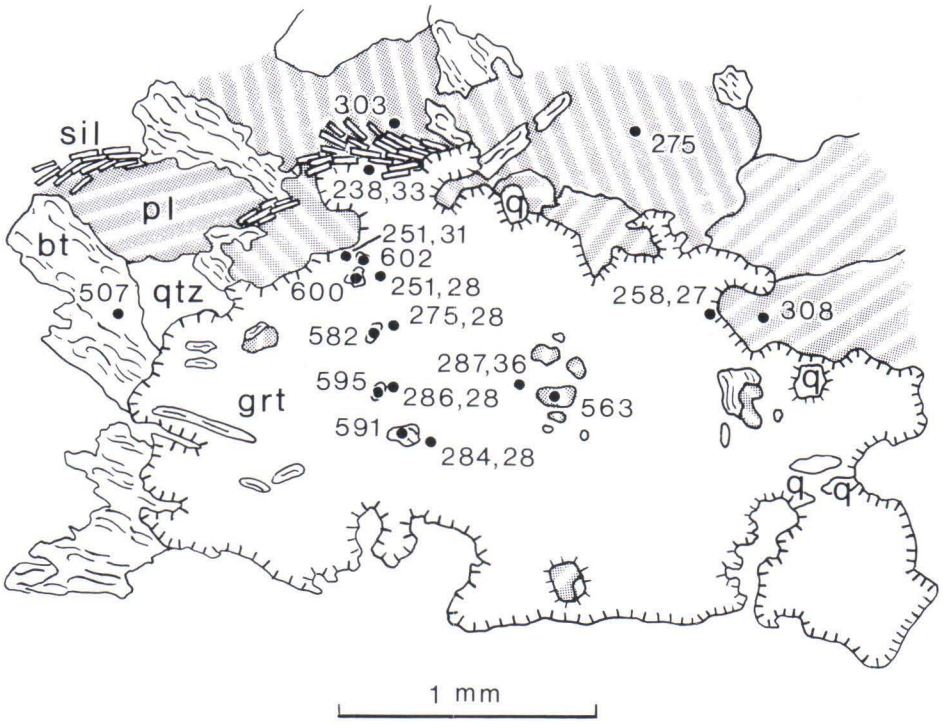

Fig. 6. Compositions of garnet and of the biotite and plagioclase inclusions in the garnet. Number referring to biotite = $X_{Mg} \times 1000$, numbers referring to garnet = X_{Mg}, $X_{Ca} \times 1000$, number referring to plagioclase = $X_{Ca} \times 1000$.

IV (sample 41a-i in Table 7) has a high Na content in contrast to that in block III (sample 49-i and 39a-i in Table 7), a fact that may be attributed to early high pressure. The anorthite content in the inclusion does not differ much from that of the matrix plagioclase in the pair analysed from block V. Of the above analysis pairs, only the garnet of 41a-i has sillimanite inclusions and hence a buffer assemblage for the barometer. The other results refer to maximum pressures. On the other hand, garnets grew during several metamorphic stages, and the PT paths of the blocks may not be alike. The calculations concerning the plagioclase inclusions were based on the estimated temperature, because the biotite inclusions analysed from the area are invariably very rich in magnesium (Fig. 6), and their composition probably represents retrograde equilibration.

PTt EVOLUTION OF THE PIELAVESI GRANULITE BLOCK

This chapter deals with the metamorphic reactions in the migmatites (group I), interpreted as semipelites, of the Pielavesi granulite block and in the garnet-cordierite-orthopyroxene rocks, originally hydrothermally altered volcanics (group II), which show abundant corona and recrystallization textures as records of crystallization history. Chemical compositions of these

rocks are given in Table 8. The classification into these two groups follows that of Marttila (1977), according to whom there are originally both volcanic and pelitic cordierite-bearing rocks in the granulite area. The mineralogy of the rocks has been described in detail by Savolahti (1966) and Marttila (1976). The mineral assemblages that probably represent the culmination of metamorphism in these rocks are listed in Table 1.

Table 8. XRF analyses of group II (52c, 55 and 59a) and group I (53 and 19) rocks.

Code	52c	55	59a	53	19
SiO_2	55.18	54.67	55.07	65.74	61.70
TiO_2	1.11	0.71	1.21	0.54	0.74
Al_2O_3	15.54	17.21	12.97	14.02	17.11
FeO tot.	21.19	18.89	21.20	6.61	7.95
MnO	0.19	0.52	0.34	0.11	0.06
MgO	5.02	6.26	5.22	2.82	3.14
CaO	1.84	1.54	2.30	2.79	1.62
Na_2O	1.65	1.63	3.55	2.59	2.45
K_2O	0.00	0.18	0.00	1.97	3.22
P_2O_5	0.49	0.04	0.06	0.06	0.05
Total	102.20	101.66	101.93	97.25	98.05

Petrography and mineral reactions

During the progressive stage the following assemblages were equilibrated in the rocks of group I:

grt-crd-bt-kfs-pl-qtz

opx-kfs-bt-pl-qtz.

Therefore, reactions (3) and

(9) bt + qtz = opx + kfs + H_2O

took place during the progressive stage. The garnet grains are euhedral or subhedral and measure 3—4 mm, on average. Many of the garnets are poikiloblastic, having a core rich in quartz and biotite inclusions but margins free from inclusions (Fig. 7). In places garnet has altered into orthopyroxene through the reaction

(8) grt + qtz = opx + pl, or

(14) grt = opx + Fe-Mg-tschermak.

Reactions (8) and (14), which produced orthopyroxene coronas around the garnet, advanced so far in some places that only a pseudomorph remains. Occasionally cordierite is rimmed with a garnet corona, and garnet with a cordierite corona, implying that reaction (5) advanced in both directions. Small granules of garnet have crystallized together with fibrolite needles on the rims of larger primary garnets when they are in contact with cordierite or with plagioclase indicating also the reaction (5) and the reaction

(15) pl = grt + sil + qtz

Garnet has altered into biotite and symplectites filled with biotite, plagioclase and quartz. Rehydration on cooling altered orthopyroxene into biotite-quartz symplectite when reaction (9) advanced from right to left. Reaction (2) altered biotite into sillimanite and occasionally into andalusite, and in places the reaction

(16) crd + sil = st + qtz

produced small staurolite crystals along the margins of the cordierite grains.

Spinel, which occurs as small inclusions in cordierite and garnet, varies from green to brown in colour.

Garnet occurs in the rocks of group II as

a) large euhedral or subhedral grains;
b) coronas around orthopyroxene grains, particularly when orthopyroxene is in contact with cordierite and plagioclase (Figs 8 and 9);
c) coronas around iron oxide or iron oxide-hercynite intergrowths (Fig. 10);
d) recrystallized along the margins of the older garnet grains, particularly when garnet is in contact with cordierite (Fig. 11). In this case, abundant magnetite was exsolved from the garnet;
e) symplectic intergrowths with biotite and quartz (Fig. 12);

f) inclusions in orthopyroxene.

Orthopyroxene occurs as

a) large euhedral or subhedral grains;
b) coronas around garnet alone or together with plagioclase (Fig. 13);
c) orthopyroxene-cordierite symplectites along the margins of garnet (Fig. 14);
d) inclusions in garnet.

Cordierite occurs as large subhedral grains sometimes filled with fine-grained opaque pigment. It is also met with as coronas rimming garnet, and as both separate grains and crd-opx-qtz symplectites.

Biotite is encountered as large flakes, which, depending on the chemical composition of the rock, are at least partly prograde. It also occurs as alteration products of garnet and orthopyroxene, forming symplectites with quartz.

Spinel occurs as intergrowths with Fe oxides or as exsolution bodies in them and as inclusions in garnet. When in contact with quartz, spinel is rimmed with a narrow cordierite corona, indicating the reaction

(4) hc + qtz = crd

The corona textures suggest that reactions (8) and (14), as well as the reaction

(17) grt + qtz + H_2O = opx + cord,

produced orthopyroxene, cordierite and garnet in the Pielavesi granulite zone.

These reactions have a gently sloping positive dP/dT, and hence they proceeded from right to left either with increasing pressure and temperature or with isobarically falling temperature. Reaction (17) is also affected by partial water pressure.

Reactions (8), (14) and (17) proceeded from left to right, altering garnet into orthopyroxene. The temporal order of the directions of the reactions is difficult to establish, but there are textures where garnet rimming orthopyroxene has altered to opx-crd symplectite. These could be interpreted as indicating that the formation of the later-generation orthopyroxene was preceded by a stage in which orthopyroxene altered to garnet.

In the contact zones of the mangerite intrusions orthopyroxenes have altered to garnet.

Sillimanite occurs in the garnet-cordierite-orthopyroxene rocks only as small acicular crystals in or along the margins of the cordierite grains, often in places where there is fine-grained recrystallized garnet or orthopyroxene. This can be attributed to reactions (5) and

(18) crd = opx + sil + qtz + H_2O.

According to experimental and calorimetric studies, the dP/dT slope of reaction (5) is gently negative (Thompson, 1976; Holdaway and Lee, 1977) or gently positive (Hutcheon *et al.*, 1974; Martignole and Sisi, 1981; Aranovich and Podlesskii, 1983). According to Newton and Wood (1979), the dP/dT of the reaction is negative for iron-rich compositions and positive for magnesium-rich compositions when the partial water pressure is higher than zero. The X_{Mg} of cordierite is generally close to 0.75 in the block, implying, according to Newton and Wood (op.cit.), that the dP/dT of the reaction was gently positive.

On account of the rare reaction (18), small acicular sillimanite grains crystallized along the margins of large hypersthene and cordierite grains, and hypersthene probably recrystallized along the margins of the older grains. According to Harris and Holland (1984), the dP/dT of this reaction, too, is gently positive. Reactions (5) and (18) proceed from left to right, also at declining partial water pressure. Since the late stage of cooling was accompanied by intense rehydration these reactions may have happened at the early stage of cooling.

When in contact with plagioclase, iron oxide is often rimmed with a garnet or symplectic garnet-quartz corona. Similar coronas have been described by Ellis and Green (1985) from the mafic granulites in Enderby Land. According to them, the reactions take place as a function of oxygen fugacity

(19) an + usp-mag_{ss} + qtz = grt + usp + O_2

(20) an + ilm-hem_{ss} + qtz = grt + ilm + O_2.

McLelland and Whitney (1977) made the same observation on the rocks of the anorthosite-

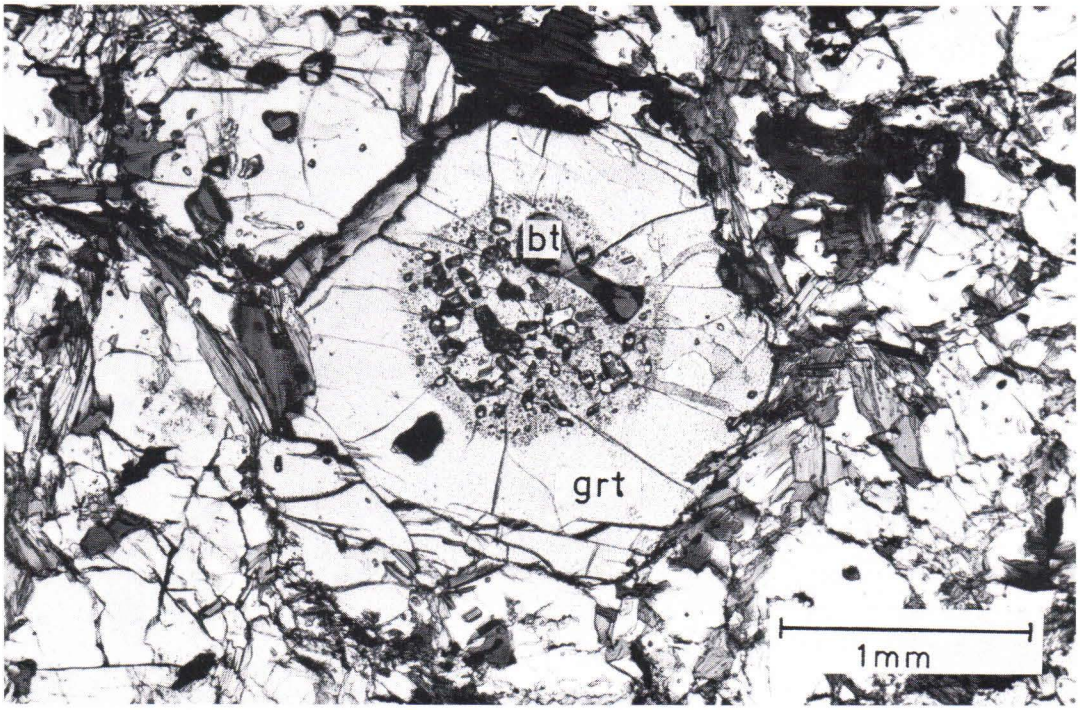

Fig. 7. Garnet with core containing quartz, plagioclase and biotite inclusions. The dusty material is composed of very small quartz grains. Outcrop 39 in Fig. 2.

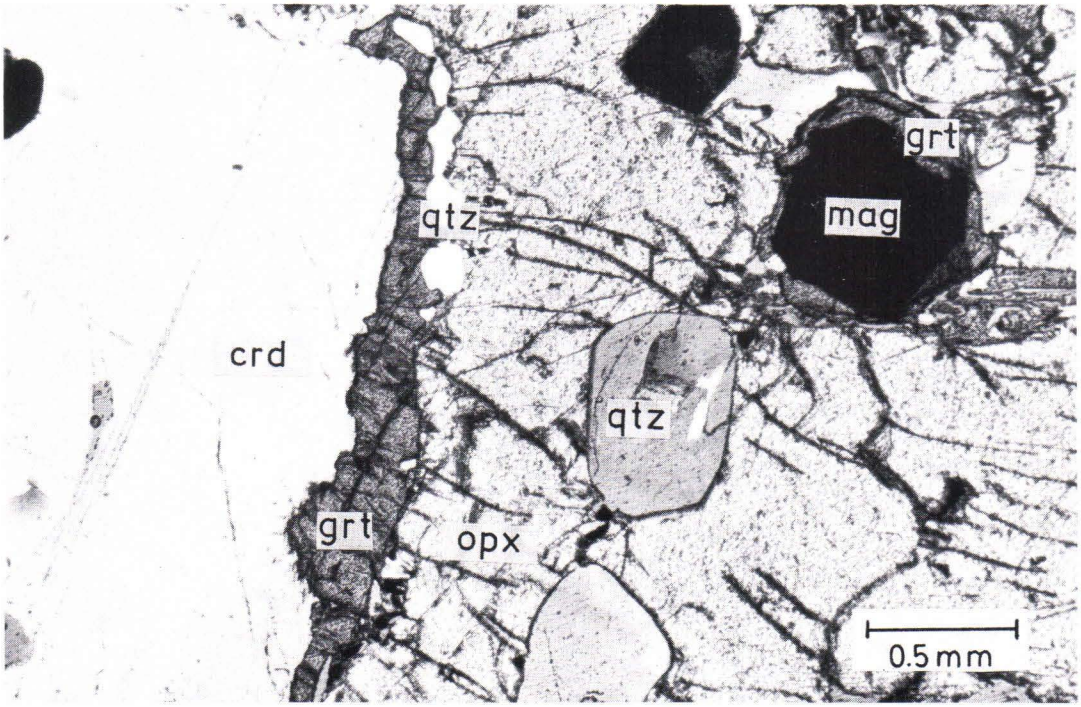

Fig. 8. Reaction (x) opx + crd = grt + qtz. Outcrop 39 in Fig. 2.

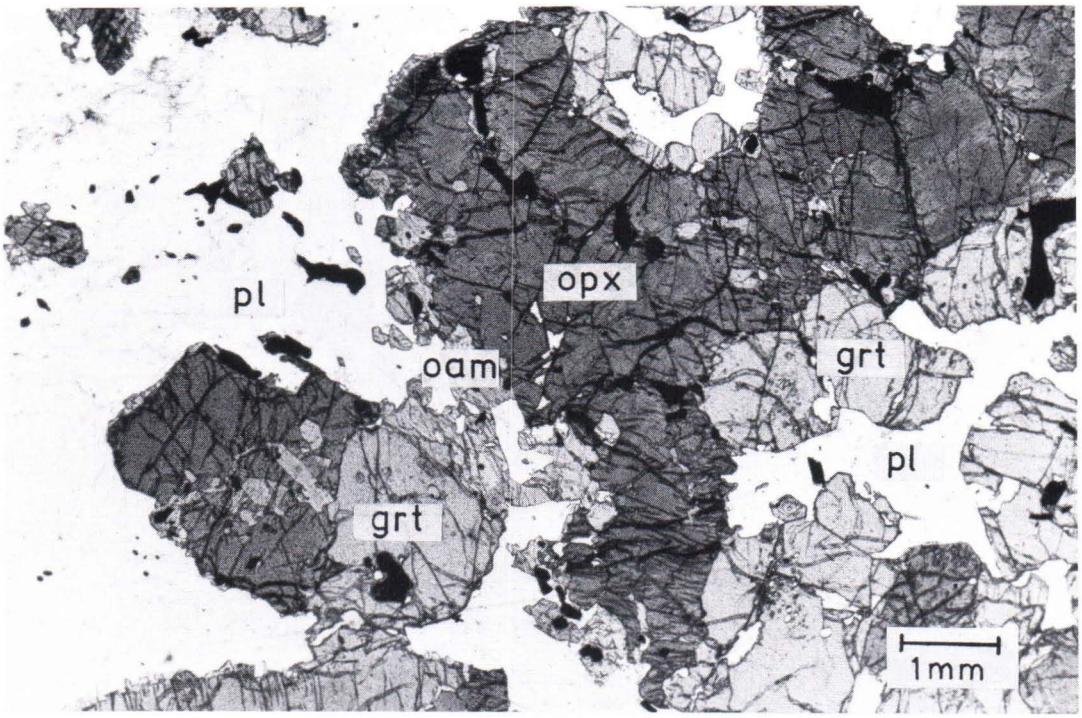

Fig. 9. Orthopyroxene altered to garnet through reaction with plagioclase. Outcrop 52 in Fig. 2.

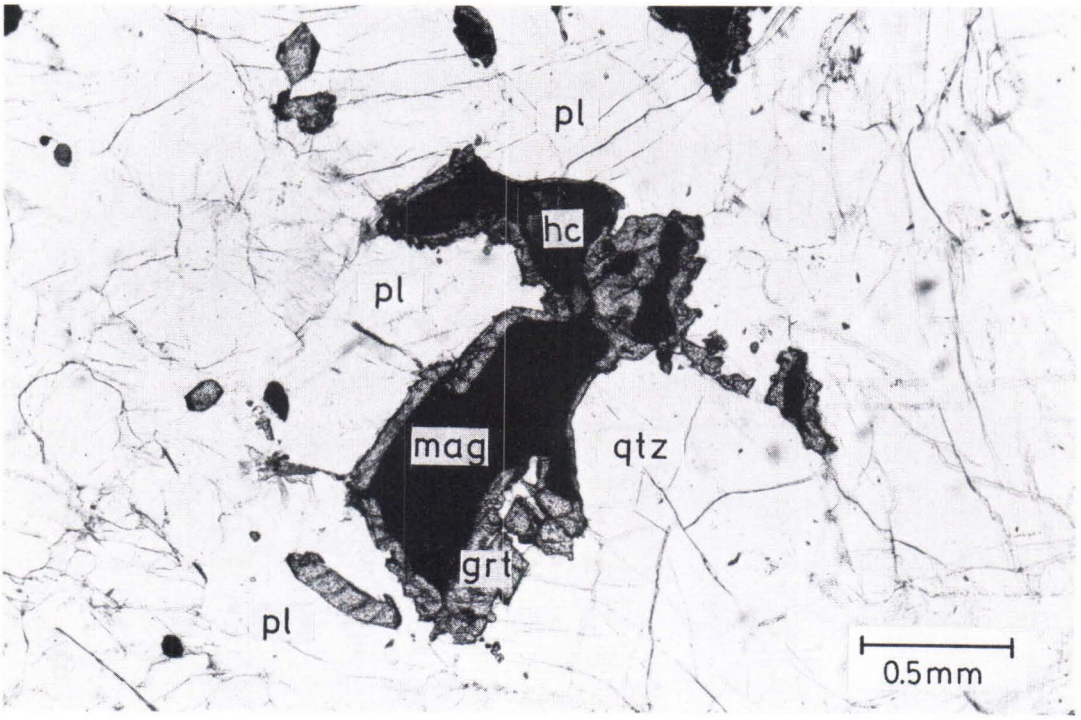

Fig. 10. Garnet corona around iron oxide. Outcrop 54 in Fig. 2.

Fig 11. Magnetite exsolutions in garnet. Outcrop 21 in Fig. 2.

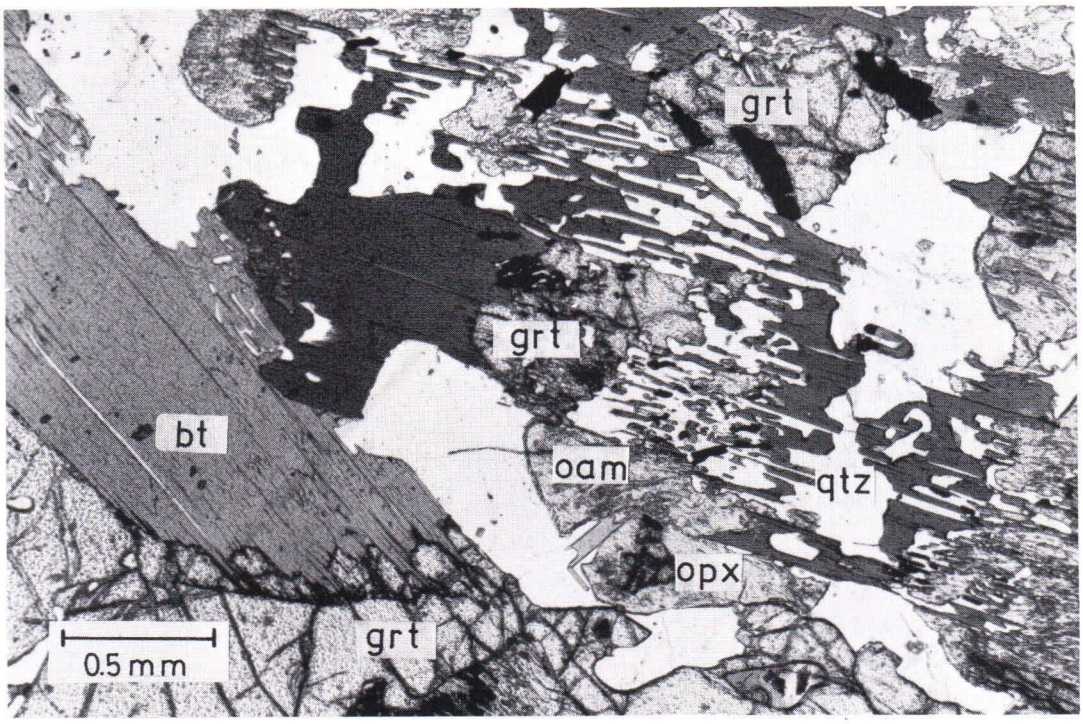

Fig 12. Garnet-biotite and biotite-orthopyroxene-orthoamphibole intergrowths. Outcrop 55 in Fig. 2.

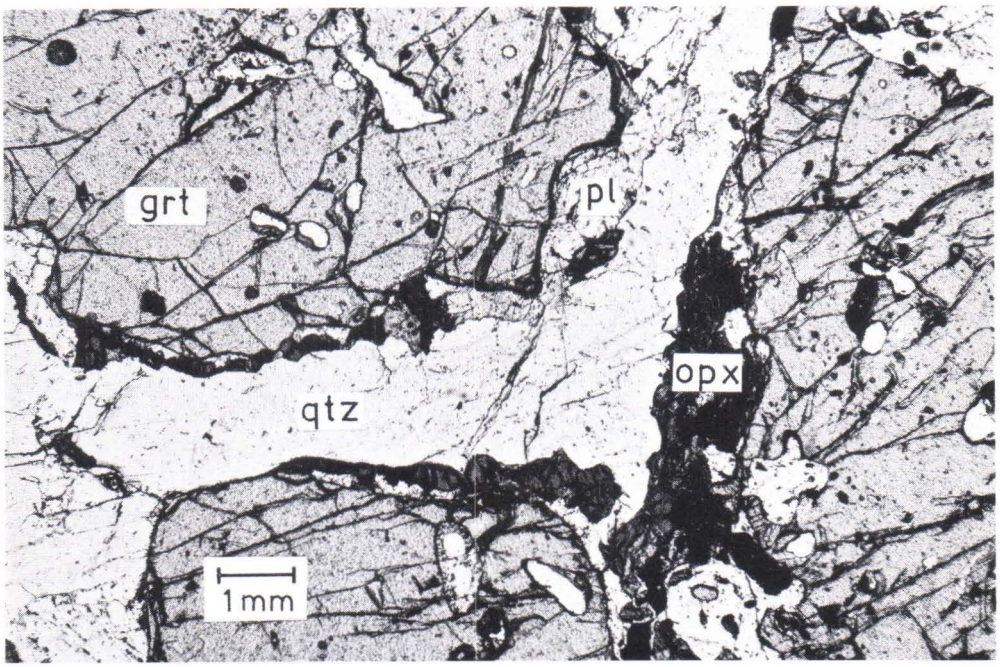

Fig. 13. Reaction grt + qtz = opx + pl. Outcrop 52 in Fig. 2.

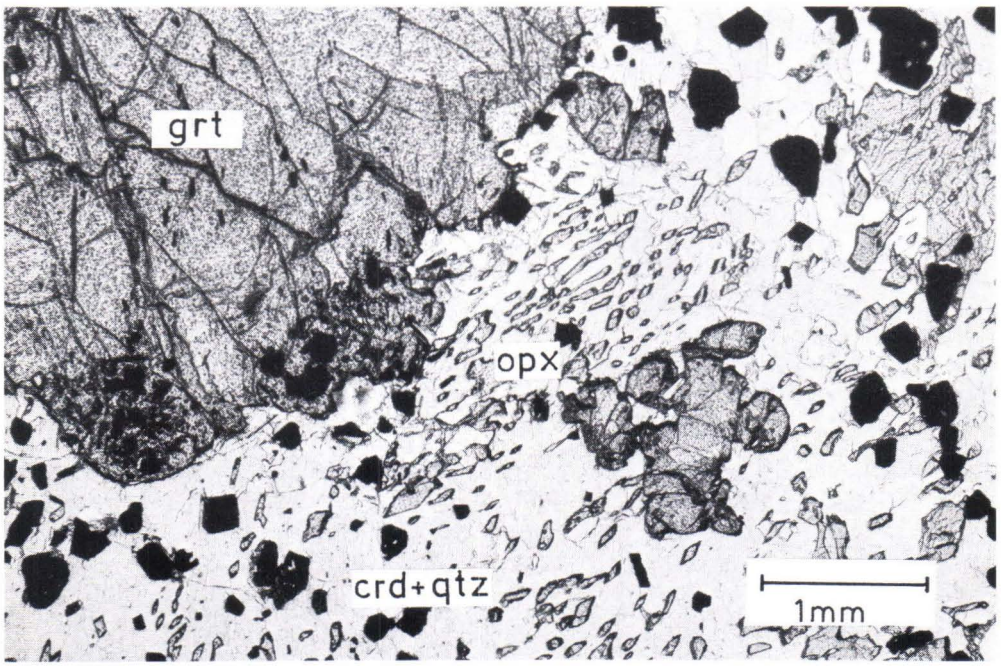

Fig. 14. Opx-crd-qtz symplectite around garnet produced by reaction grt + qtz = opx + crd. Outcrop 52 in Fig. 2.

charnockite series in the Adirondacks, but they attributed the phenomenon to partial reactions in which plagioclase and orthopyroxene first react with each other, thereby forming garnet. The extra iron needed for the formation of garnet derives from iron oxide. The reaction liberates Mg ions from orthopyroxene, which then participate in the reaction between plagioclase and iron oxide, generating a Ca-Mg-Fe garnet corona around the oxide.

Even when not in contact with plagioclase, the iron oxide-spinel intergrowths are rimmed with a garnet corona. A possible reaction is then

(21) mag + hc + qtz = grt + O_2.

When orthopyroxene is in contact with iron oxide, garnet has often crystallized between them as a result of the reaction

(22) mag + Fe-ts + qtz = grt + O_2.

When garnet has crystallized along the margins of cordierite through reaction (5), it contains small magnetite inclusions averaging 3—5 μm in size (Fig. 11). The same phenomenon is shown by the fine-grained garnet grains, which have often crystallized along the margins of the older garnet grains in group I rocks as a result of reaction (15).

In places, several magnetite exolution zones have grown in garnet (Fig. 11). These exolutions are products of the reaction

(23) alm + O_2 = prp + mag

as the pyrope content of garnet increases when magnetite is exsolved.

Unlike reactions (19—22), which advance from left to right at declining partial oxygen pressure, reaction (23) binds oxygen, and thus indicates increasing oxygen fugacity.

During rehydration, the orthopyroxene of the group II rocks was altered to amphibole along the margins by the reaction

(24) opx + qtz + H_2O = ath or cum.

The signature of the reaction is recognizable virtually throughout the granulite area.

Mineral chemistry

Orthopyroxene

The large orthopyroxene grains are enveloped by a rim about 0.25 mm wide in which X_{Mg} (Mg/Mg + Fe) increases and X_{Al} (Al/2) decreases (Fig. 15). The change is greatest in the orthopyroxene in contact with garnet, suggesting diffusion on cooling. This is the only marked zoning shown by the orthopyroxenes. In the large orthopyroxene grains analysed, X_{Mg} varies from 0.50 to 0.59. The magnesium contents are the same, irrespective of whether the rock belongs to group I or II. The average magnesium contents are higher in the orthopyroxene coronas, less than 2 mm wide, that rim garnet, their X_{Mg} varying from 0.55 to 0.62. Figure 16 illustrates the composition profile of a corona. The mole fraction of magnesium is lowest, about 0.46—0.55 (Table 17), in the pyroxenes, that were analysed from close to the contacts of mangerites. In the contact zones of mangerites, X_{Al} is about 0.03—0.10; elsewhere in the granulite zone it is about 0.11—0.17 (Table 17). The X_{Al} correlates with the composition of garnet in that it declines with the increase in the grossular component, as reported by Harley (1985), but increases with the increase in the pyrope component. Table 9 lists some orthopyroxene compositions.

Garnet

The large garnet grains, over 5 mm in diameter, are fairly rich in magnesium. The composition depends on grain size rather than on whether the rock belongs to group I or II; in the

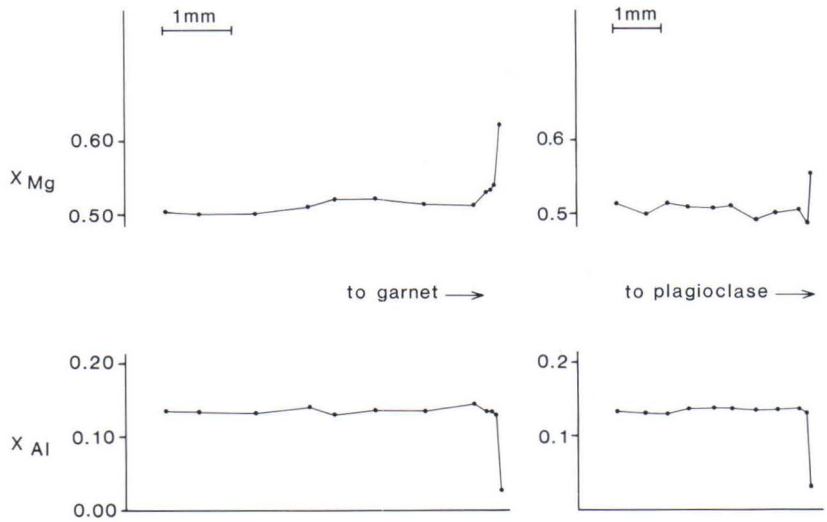

Fig. 15. Composition profile of orthopyroxene from core to rim. Sample 55a—c.

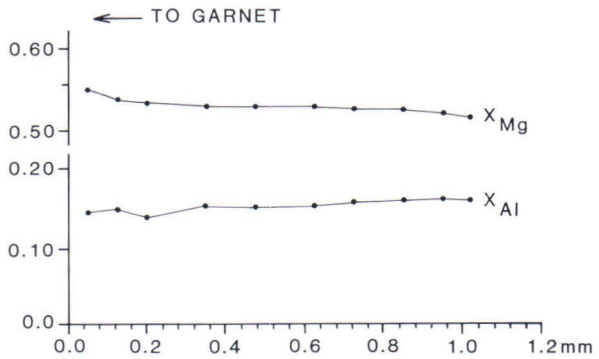

Fig. 16. Composition profile of the orthopyroxene corona around garnet across the grain. Sample 52b.

former, the mole fraction of magnesium averages 0.27—0.29, and in the latter 0.30—0.35. However, compositions exceeding 0.30 have been recorded from the largest garnet grains, even in mica gneisses (group I), whose garnets tend to be smaller on the whole. The garnet grains exhibit zoning with X_{Mg}, X_{Fe} and X_{Ca} varying within a few hundredths. Outermost there is a diffusion rim, a quarter of a millimetre wide, in which X_{Mg} declines consistently. The zoning of the garnets is illustrated in Figs. 17a—d. A feature typical of many grains is that the Mg content first decreases from the core towards the rim and then rises again close to the margin.

The highest pyrope contents of the garnet coronas exceed 0.30. However, the composition profile differs from that of the large primary garnet grains, as the magnesium content is highest in the rim farthest from the orthopyroxene (Fig. 17b). Zoning like this is ascribed to the growth of garnet at the expense of orthopyroxene. Closest to orthopyroxene the mole fraction of magnesium declines steeply as in the primary garnets, implying diffusion after the grain had ceased to grow. The high magnesium contents of the garnet coronas show that the reaction start-

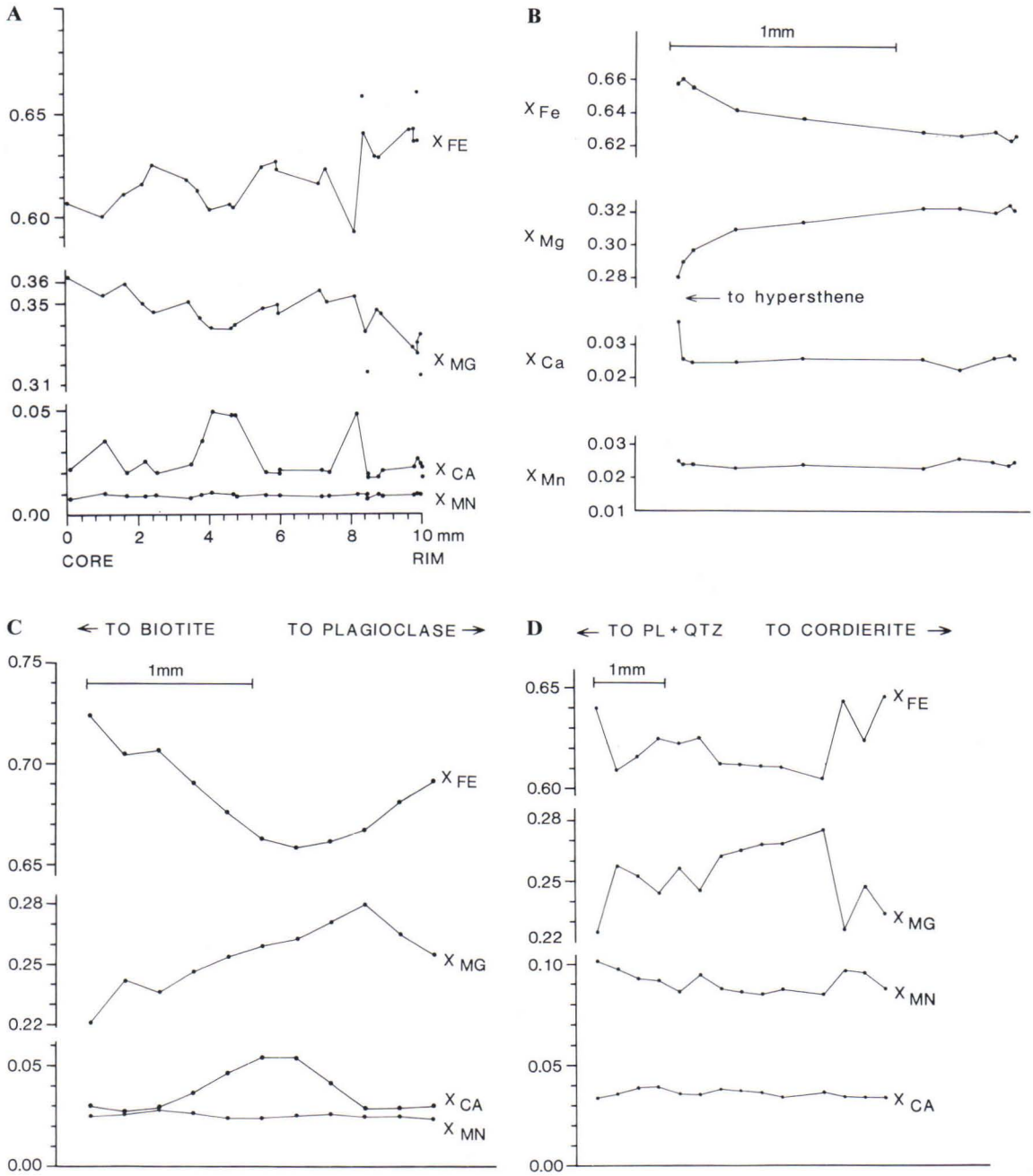

Fig. 17. Zoning in garnets. a) Garnet 52b from core to rim, b) garnet corona 55a—c on the margin of orthopyroxene across the grain, c) garnet 49 across the grain, d) garnet 50 across the grain.

ed at fairly high temperatures. The magnesium content of the garnet corona that crystallized at the margins of the more iron-rich orthopyroxene close to the contact of the mangerites is lower, about 0.2.

The mole fraction of magnesium in the garnet

inclusion in orthopyroxene is lower than in the grains outside the orthopyroxene, probably because of retrograde diffusion.

The fine-grained garnet produced by reaction (5) is also fairly rich in magnesium; according to the only analysis made of such a grain, the X_{Mg} of the garnet is 0.33. Cordierite, too, of which garnet is an alteration product, contains abundant magnesium and has X_{Mg} 0.83.

The calcium and manganese contents of the garnets of both lithological groups are low, the mole fractions usually being less than 0.05. However, zones richer in are registered in the composition profile in Figs. 17a and 17c. A point in the garnet corona around the magnetite analysed showed X_{Ca} 0.06, X_{Mg} 0.17 and X_{Mn} 0.04. The sample was taken from close to the mangerite contact (outcrop 59, Fig. 2).

A garnet grain with magnetite exsolutions in the margins was submitted to analyses by assaying points in the core and on the margins of the grain. In the core, X_{Mg} was 0.29 and on the margin 0.31. The X_{Ca} decreases from 0.03 in the core to 0.003 on the margin.

Garnet analyses are in Table 10.

Cordierite

The cordierite in contact with garnet is richer in Mg (X_{Mg} = 0.77—0.83) than the matrix cordierite (X_{Mg} = c. 0.75, X_{Mg} = Mg/Mg + Fe). The compositions of cordierite are fairly similar in the rocks of groups I and II (Table 11).

Biotite

In biotite, X_{Mg} (X_{Mg} = Mg/Mg + Fe + Mn + Ti + Al^{iv}) varies from 0.5 to 0.6. The Mg contents are highest, over 0.6, in the biotites that occur as inclusions in garnet (Fig. 6). The TiO_2 content fluctuates between 3 and 5% (Table 12). The biotite inclusions in garnet have normally TiO_2 values from 2.2 to 3%, which are lower than those in the matrix biotite. Hölttä (1986) made a similar observation in the Turku granulite area.

Plagioclase

The calcium contents of plagioclase and garnet depend on the whole-rock calcium content. In the mangerite contacts the anorthite content of the plagioclase in relation to the grossularite component of the garnet is, on average, higher than outside the contact zones. Figure 18 illustrates a zonal plagioclase grain in contact with orthopyroxene, which have reacted giving rise to garnet and quartz. The Ca content declines towards the orthopyroxene, implying that plagioclase has transferred calcium to garnet. In the rocks of group I the plagioclase inclusions in garnet are richer in calcium than is the matrix plagioclase (Table 7, Fig. 6). Table 13 lists the compositions of some plagioclases.

Orthoamphibole

Orthoamphiboles that are alteration products of orthopyroxene are similar to the host mineral in composition. The primary orthoamphibole is aluminium-rich gedrite (Table 14).

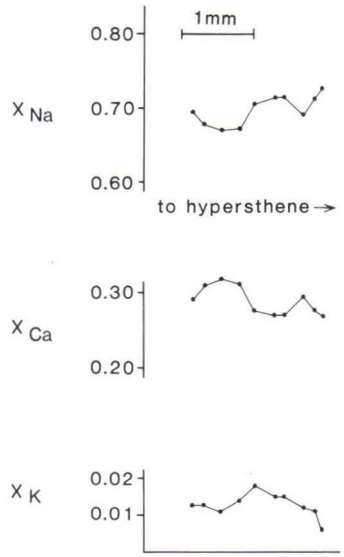

Fig. 18. Zoning in plagioclase. Sample 55a—c across the grain.

Spinel

Hercynitic and gahnitic spinels in contact with iron oxide were analysed from the rocks of group II. X_{Fe} varies from 0.40 to 0.67, and X_{Zn} from 0.01 to 0.42 (Table 15).

Iron oxides

Magnetite contains little of any components except iron (Table 16). However, the titanium content of the magnetite in contact with ilmenite is ten times higher than what it is in the rest of the grain. The margin of ilmenite in contact with magnetite is also richer in titanium than in the rest of the grain.

PT determinations

Table 17 gives temperature and pressure values determined with garnet-orthopyroxene thermometers (Harley, 1984a; Perchuk *et al.*, 1985; Sen and Bhattacharya, 1984), garnet-plagioclase-orthopyroxene-quartz barometers (Newton and Perkins, 1982; Perkins and Chipera, 1985) and the garnet-orthopyroxene barometer (Harley, 1984b). The pressures according to Perkins and Chipera were calculated with their program NEWBAR.

The results have been divided into four groups on the basis of metamorphic reactions. The highest temperatures and pressures were obtained from the compositions of the cores of the large grains. All the temperatures given by the thermometers of Harley (1984a) (723—883°C) are consistent with those of Perchuk *et al.* (1985) (743—850°C), whereas those given by the thermometer of Sen and Bhattacharya (1984) (755—1050°C) are improbably high. The pressures in-

Table 9. Orthopyroxene analyses. Analyses 52, 52a, 53, 54 ja 55 are from the cores of large grains; 54b and 52b refer to the opx coronas on garnet. The remaining six analyses are core compositions from the contact zones of mangerites. Analysis 59b is from an alteration product of garnet. The number after the code indicates the distance in metres from the contact of the mangerite intrusion.

Code	52	52a	53	54	55	54b	52b	56—3m.	57—100m.	58—200m.	59a—200m.	59b—200m.	59c—200m.
SiO_2	48.19	47.23	50.70	47.99	49.62	47.56	48.62	49.37	48.75	47.78	46.79	48.18	49.42
TiO_2	0.14	0.14	0.09	0.09	0.16	0.12	0.09	0.16	0.13	0.21	0.18	0.05	0.02
Al_2O_3	6.72	7.37	2.59	6.43	5.81	7.26	6.07	3.66	3.70	3.70	4.47	2.92	3.88
FeO	25.78	26.09	28.80	24.38	27.61	24.16	24.25	31.00	27.36	29.11	30.57	29.48	30.78
MnO	0.18	0.17	0.46	0.61	0.33	0.55	0.05	0.26	0.37	0.48	0.67	0.50	0.60
MgO	18.05	17.75	17.60	19.06	17.89	18.75	19.90	15.30	17.38	15.95	14.80	16.46	15.65
CaO	0.05	0.04	0.17	0.05	0.13	0.06	0.05	0.13	0.17	0.18	0.12	0.09	0.11
Na_2O	0.00	0.00	0.05	0.08	0.01	0.02	0.02	0.01	0.02	0.01	0.02	0.00	0.05
K_2O	0.00	0.00	0.02	0.03	0.00	0.00	0.01	0.00	0.00	0.01	0.01	0.00	0.00
V_2O_3	0.03	0.03	0.03	0.01	0.06	0.01	0.01	0.06	0.07	0.13	0.01	0.01	0.02
Cr_2O_3	0.00	0.01	0.01	0.00	0.01	0.02	0.00	0.04	0.04	0.13	0.01	0.00	0.02
NiO	0.02	0.00	0.00	0.04	0.00	0.04	0.00	0.01	0.00	0.00	0.00	0.00	0.00
Total	99.16	98.83	100.53	98.75	101.62	98.55	99.07	100.01	98.01	97.69	97.66	97.68	100.55
Number of cations based on 6 oxygens													
Si	1.8392	1.8141	1.9362	1.8344	1.8605	1.8188	1.8442	1.9151	1.9032	1.8926	1.8700	1.9105	1.9065
Ti	0.0040	0.0040	0.0026	0.0025	0.0045	0.0033	0.0025	0.0048	0.0038	0.0064	0.0055	0.0014	0.0007
Al	0.3025	0.3336	0.1166	0.2896	0.2567	0.3270	0.2711	0.1671	0.1705	0.1729	0.2105	0.1363	0.1766
Fe	0.8230	0.8380	0.9198	0.7792	0.8658	0.7727	0.7691	1.0054	0.8933	0.9644	1.0217	0.9778	0.9930
Mn	0.0058	0.0056	0.0150	0.0196	0.0105	0.0177	0.0017	0.0087	0.0123	0.0160	0.0225	0.0166	0.0197
Mg	1.0267	1.0165	1.0016	1.0857	0.9999	1.0690	1.1251	0.8848	1.0112	0.9419	0.8817	0.9730	0.8998
Ca	0.0022	0.0015	0.0070	0.0021	0.0050	0.0025	0.0021	0.0054	0.0073	0.0078	0.0050	0.0037	0.0045
Na	0.0004	0.0000	0.0038	0.0060	0.0009	0.0013	0.0013	0.0011	0.0015	0.0005	0.0018	0.0000	0.0037
K	0.0000	0.0000	0.0010	0.0013	0.0000	0.0000	0.0005	0.0000	0.0000	0.0005	0.0006	0.0000	0.0000
V	0.0009	0.0009	0.0008	0.0003	0.0018	0.0003	0.0005	0.0017	0.0022	0.0040	0.0004	0.0003	0.0006
Cr	0.0000	0.0004	0.0004	0.0000	0.0004	0.0007	0.0000	0.0011	0.0014	0.0040	0.0003	0.0001	0.0005
Ni	0.0005	0.0000	0.0000	0.0012	0.0000	0.0012	0.0001	0.0004	0.0000	0.0000	0.0000	0.0000	0.0001

Table 10. Garnet analyses. 19a, 52a, 54b, 52b, 52b and 53 are large primary garnets, 52, 54 and 55 refer to the alteration products of orthopyroxene; and 56—59 are garnets from the contact aureoles of mangerite intrusions. Analyses 19a and 56 are from the group I rocks and the remaining analyses from the group II rocks. The letter c refers to the composition of the core and the letter r to that of the rim; when these are absent the analysis refers to the core. The number succeeding the code denotes the distance in metres from the mangerite contact. n.d. = not determined.

Code	19a—c	19a—r	52a	54b	52b—c	52b—r	53	52	54	55	56—3m.	57—100m.	58—2m.	59a—200m.	59b—200m.	59c—200m.
SiO_2	38.50	37.90	39.17	38.12	38.45	38.02	38.90	39.17	38.53	39.70	38.34	37.99	36.99	37.05	36.82	38.64
TiO_2	0.03	0.07	0.01	0.02	0.02	0.00	0.01	0.00	0.02	0.07	0.02	0.03	0.06	0.05	0.09	0.02
Al_2O_2	22.00	22.00	21.81	21.53	21.77	21.39	22.19	21.86	21.67	22.37	21.90	21.57	21.18	21.00	21.02	21.81
FeO	27.30	28.70	28.09	29.52	28.41	29.22	29.90	29.94	28.59	29.32	31.86	29.83	31.46	32.05	33.04	31.86
MnO	0.55	0.57	0.47	2.76	0.41	0.37	1.64	0.56	2.53	1.04	0.83	1.16	1.23	2.09	1.92	2.20
MgO	9.60	9.33	9.31	7.27	9.46	8.12	7.29	8.28	8.07	8.72	6.12	7.81	6.20	5.55	4.80	5.61
CaO	1.27	1.16	1.14	0.68	0.78	0.72	1.55	0.63	0.64	0.96	1.07	1.15	1.33	1.06	1.07	0.99
Na_2O	0.01	0.04	0.00	0.02	0.05	0.07	0.02	0.02	0.00	0.02	0.02	0.01	0.00	0.00	0.02	0.02
K_2O	0.00	0.02	0.00	0.00	0.01	0.04	0.00	0.00	0.01	0.00	0.01	0.00	0.00	0.00	0.01	0.00
V_2O_3	n.d.	n.d.	0.00	0.02	0.02	0.00	0.01	0.03	0.01	0.03	0.05	0.04	0.03	0.00	0.02	0.01
Cr_2O_3	n.d.	n.d.	0.01	0.00	0.00	0.03	0.00	0.00	0.00	0.00	0.06	0.05	0.01	0.00	0.00	0.00
NiO	n.d.	n.d.	0.00	0.01	0.00	0.02	0.00	0.01	0.00	0.00	0.00	0.00	0.00	0.02	0.00	0.00
Total	99.26	99.79	100.02	99.94	99.38	97.96	101.51	100.51	100.07	102.23	100.29	99.63	98.49	98.89	98.83	101.18
Number of cations based on 12 oxygenes																
Si	2.9823	2.9440	3.0149	2.9904	2.9853	3.0098	2.9921	3.0212	2.9987	3.0050	3.0029	2.9785	2.9675	2.9775	2.9740	3.0142
Ti	0.0017	0.0041	0.0008	0.0011	0.0014	0.0002	0.0006	0.0000	0.0012	0.0040	0.0011	0.0015	0.0037	0.0028	0.0054	0.0013
Al	2.0085	2.0141	1.9777	1.9904	1.9925	1.9957	2.0116	1.9868	1.9879	1.9957	2.0219	1.9926	2.0029	1.9890	2.0014	2.0049
Fe	1.7685	1.8644	1.8081	1.9366	1.8447	1.9343	1.9234	1.9312	1.8604	1.8558	2.0868	1.9558	2.1105	2.1544	2.2321	2.0784
Mn	0.0361	0.0375	0.0308	0.1834	0.0268	0.0247	0.1066	0.0367	0.1666	0.0669	0.0553	0.0768	0.0836	0.1423	0.1317	0.1457
Mg	1.1084	1.0802	1.0679	0.8500	1.0953	0.9579	0.8363	0.9523	0.9360	0.9836	0.7150	0.9126	0.7409	0.6651	0.5779	0.6523
Ca	0.1054	0.0965	0.0942	0.0567	0.0651	0.0609	0.1281	0.0521	0.0531	0.0779	0.0900	0.0970	0.1144	0.0915	0.0928	0.0826
Na	0.0015	0.0060	0.0000	0.0027	0.0078	0.0101	0.0031	0.0028	0.0000	0.0029	0.0027	0.0015	0.0000	0.0008	0.0031	0.0035
K	0.0000	0.0020	0.0000	0.0000	0.0007	0.0042	0.0001	0.0004	0.0012	0.0000	0.0015	0.0000	0.0003	0.0000	0.0009	0.0000
V	n.d.	n.d.	0.0002	0.0015	0.0011	0.0000	0.0004	0.0017	0.0007	0.0017	0.0028	0.0022	0.0019	0.0002	0.0014	0.0007
Cr	n.d.	n.d.	0.0005	0.0000	0.0000	0.0000	0.0003	0.0000	0.0003	0.0001	0.0040	0.0031	0.0004	0.0003	0.0003	0.0000
Ni	n.d.	n.d.	0.0000	0.0009	0.0000	0.0015	0.0000	0.0009	0.0000	0.0001	0.0000	0.0000	0.0000	0.0014	0.0000	0.0000

Table 11. Cordierite analyses. c = core, r = rim of grain n.d. = not determined. 19a is from group I rock and the others from group II.

	52	19a-c	19a-r	54	20
SiO_2	49.60	49.00	49.20	49.26	47.94
TiO_2	0.01	0.00	0.01	0.00	0.00
Al_2O_3	34.30	33.20	33.40	33.39	32.03
FeO	5.39	5.25	4.71	3.99	4.87
MnO	0.01	0.01	0.06	0.06	0.03
MgO	10.90	10.60	10.80	10.95	10.13
CaO	0.00	0.01	0.04	0.00	0.00
Na_2O	0.08	0.00	0.04	0.04	0.06
K_2O	0.00	0.00	0.00	0.01	0.00
V_2O_3	n.d.	n.d.	n.d.	0.02	0.00
Cr_2O_3	n.d.	n.d.	n.d.	0.00	0.02
NiO	n.d.	n.d.	n.d.	0.00	0.00
Total	100.29	98.07	98.26	97.71	95.07
Number of cations based on 18 oxygens					
Si	4.9410	4.9858	4.9856	5.0006	5.0235
Ti	0.0007	0.0000	0.0008	0.0000	0.0000
Al	4.0270	3.9814	3.9889	3.9947	3.9560
Fe	0.4490	0.4467	0.3991	0.3387	0.4266
Mn	0.0008	0.0009	0.0051	0.0048	0.0022
Mg	1.6184	1.6076	1.6312	1.6567	1.5815
Ca	0.0000	0.0011	0.0043	0.0000	0.0000
Na	0.0155	0.0000	0.0079	0.0071	0.0114
K	0.0000	0.0000	0.0000	0.0017	0.0000
V	n.d.	n.d.	n.d.	0.0015	0.0000
Cr	n.d.	n.d.	n.d.	0.0000	0.0019
Ni	n.d.	n.d.	n.d.	0.0000	0.0000

Table 12. Biotite analyses. cg = in contact with garnet, m = matrix biotite, i = inclusion in garnet, n.d. = not determined.

	19a-cg	19a-m	19a-i	57-m	20-m
SiO_2	37.30	36.60	38.30	35.19	35.27
TiO_2	4.51	4.54	4.26	4.88	3.54
Al_2O_3	16.40	16.40	16.61	14.83	15.98
FeO	12.10	14.00	10.20	16.33	14.16
MnO	0.02	0.00	0.00	0.05	0.02
MgO	14.60	13.90	15.43	12.40	13.66
CaO	0.00	0.00	0.05	0.00	0.06
Na_2O	0.06	0.04	0.18	0.04	0.23
K_2O	9.71	9.60	9.35	9.49	8.85
V_2O_3	n.d.	n.d.	0.11	0.18	0.12
Cr_2O_3	n.d.	n.d.	0.06	0.12	0.00
NiO	n.d.	n.d.	0.01	0.03	0.00
Total	94.70	95.08	94.55	93.54	91.88
Number of cations based on 22 oxygens					
Si	5.5250	5.4549	5.6064	5.4292	5.4490
Ti	0.5024	0.5089	0.4689	0.5664	0.4110
Al	1.4989	1.7450	1.2481	2.1070	1.8291
Fe	2.8630	2.8808	2.8658	2.6966	2.9095
Mn	0.0025	0.0000	0.0000	0.0061	0.0031
Mg	3.2234	3.0879	3.3658	2.8522	3.1446
Ca	0.0000	0.0000	0.0071	0.0000	0.0108
Na	0.0172	0.0116	0.0508	0.0120	0.0677
K	1.8347	1.8252	1.7449	1.8679	1.7435
V	n.d.	n.d.	0.0129	0.0228	0.0151
Cr	n.d.	n.d.	0.0074	0.0140	0.0000
Ni	n.d.	n.d.	0.0013	0.0035	0.0000

dicated by the grt-opx-pl-qtz barometer average 5.3 ± 0.6 kb. However, the sample in which the pyrope content of the garnet was the highest shows a pressure exceeding 8 kb. The results given by Harley's barometer exhibit a high scatter due to the great variation in the aluminium content of orthopyroxene. At the lowest aluminium contents the pressures of all groups are improbably high.

The second group contains the PT determinations based on the composition of orthopyroxene and the garnet altered from it. The analytical data on orthopyroxene were obtained from close to the margins, not, however, from the outermost diffusion rim, which may have formed on cooling after the net transfer reaction had stopped. The pressures (4.7 ± 0.8 kb) and temperatures (659—881°C) are only slightly lower, on average, than in the first group. Since the garnet that is an alteration product of orthopyroxene is fairly rich in magnesium, the reaction must have started at high temperatures. Determinations 55a, 55b and 55c listed in Table 17 were based on the compositions of the garnet, orthopyroxene and plagioclase shown in Figs 17b, 15 and 18. The first determination ($T_1 = 881°C$, $P_2 = 6.0$ kb in Table 17) was based on the compositions of the core of the orthopyroxene and the outermost rim of garnet and plagioclase; the second ($T_1 = 751°C$, $P_2 = 4.5$ kb), on the compositions of orthopyroxene close to the margin and cores of garnet and plagioclase; and the third ($T_1 = 614°C$, $P_2 = 4.8$ kb), on the compositions of the innermost rims.

Table 13. Plagioclase analyses. 54b and 52b refer to the plagioclase coronas produced by the reaction grt + qtz = opx + pl; 56—59 are from the mangerite contacts; the number after the code denotes the distance in metres from the contact.

Code	19a	55	53	54	52	52a	54b	52b	58—2m	57—100m	59c—200m	59b—200m	59a—200m	56—3m
SiO_2	61.00	60.84	60.03	61.97	62.10	61.38	62.22	60.48	57.27	57.45	61.26	59.33	59.39	59.46
TiO_2	0.01	0.03	0.00	0.02	0.02	0.00	0.01	0.00	0.01	0.04	0.04	0.00	0.01	0.01
Al_2O_3	25.40	25.02	25.18	22.28	22.88	22.88	22.46	23.00	24.28	24.54	24.20	22.93	22.70	24.66
FeO	0.03	0.03	0.02	0.05	0.03	0.03	0.03	0.19	0.08	0.00	0.19	0.07	0.04	0.06
MnO	0.00	0.00	0.00	0.00	0.00	0.00	0.00	0.00	0.00	0.02	0.00	0.01	0.00	0.01
MgO	0.00	0.00	0.00	0.00	0.00	0.00	0.00	0.00	0.00	0.00	0.00	0.00	0.00	0.00
CaO	7.01	6.41	6.86	3.91	4.45	4.55	3.97	4.92	6.99	7.23	5.73	5.28	5.31	6.43
Na_2O	7.34	7.87	7.78	9.32	9.19	9.05	9.32	9.07	7.34	7.33	8.35	8.60	8.50	7.55
K_2O	0.09	0.16	0.33	0.46	0.09	0.09	0.36	0.05	0.23	0.24	0.19	0.15	0.22	0.22
V_2O_3	n.d.	0.01	0.01	0.01	0.00	0.01	0.02	0.01	0.01	0.00	0.01	0.00	0.00	0.01
Cr_2O_3	n.d.	0.00	0.01	0.00	0.01	0.00	0.03	0.00	0.02	0.00	0.00	0.00	0.00	0.00
NiO	n.d.	0.00	0.00	0.01	0.03	0.00	0.00	0.02	0.01	0.00	0.00	0.01	0.04	0.00
Total	100.88	100.37	100.23	98.04	98.79	97.92	98.42	97.73	96.25	96.86	99.98	96.39	96.20	98.43
Number of ions based on 8 oxygens.														
Si	2.6868	2.6951	2.6721	2.8017	2.7837	2.7770	2.8002	2.7507	2.6583	2.6510	2.7241	2.7377	2.7455	2.6880
Ti	0.0003	0.0009	0.0000	0.0006	0.0006	0.0002	0.0004	0.0000	0.0005	0.0014	0.0014	0.0000	0.0002	0.0005
Al	1.3186	1.3062	1.3208	1.1873	1.2086	1.2155	1.1911	1.2329	1.3281	1.3344	1.2684	1.2470	1.2369	1.3139
Fe	0.0011	0.0011	0.0007	0.0021	0.0010	0.0012	0.0012	0.0071	0.0030	0.0000	0.0069	0.0028	0.0015	0.0023
Mn	0.0000	0.0000	0.0000	0.0002	0.0000	0.0000	0.0000	0.0000	0.0000	0.0008	0.0001	0.0005	0.0000	0.0003
Mg	0.0000	0.0000	0.0000	0.0001	0.0000	0.0002	0.0000	0.0000	0.0000	0.0003	0.0002	0.0000	0.0000	0.0000
Ca	0.3308	0.3043	0.3274	0.1894	0.2140	0.2207	0.1915	0.2397	0.3478	0.3576	0.2731	0.2613	0.2628	0.3115
Na	0.6268	0.6758	0.6718	0.8170	0.7987	0.7937	0.8132	0.7996	0.6602	0.6554	0.7199	0.7691	0.7622	0.6615
K	0.0051	0.0092	0.0189	0.0266	0.0050	0.0055	0.0206	0.0027	0.0139	0.0143	0.0106	0.0088	0.0127	0.0127
V	n.d.	0.0005	0.0005	0.0003	0.0000	0.0004	0.0007	0.0004	0.0003	0.0000	0.0005	0.0001	0.0001	0.0005
Cr	n.d.	0.0000	0.0002	0.0000	0.0004	0.0000	0.0009	0.0000	0.0009	0.0000	0.0000	0.0000	0.0000	0.0002
Ni	n.d.	0.0000	0.0000	0.0003	0.0011	0.0000	0.0000	0.0007	0.0005	0.0000	0.0000	0.0003	0.0014	0.0002

Table 14. Compositions of orthoamphiboles. 52 refers to gedrite in contact with garnet; 52a is a gedrite inclusion in garnet; and 13 and 60 refer to the alteration products of orthopyroxene.

Code	52	52a	13	60
SiO_2	37.90	38.17	52.25	52.52
TiO_2	0.46	0.29	0.10	0.08
Al_2O_3	16.91	16.04	4.79	4.86
FeO	18.23	17.55	23.41	19.92
MnO	0.09	0.09	0.21	0.14
MgO	16.33	17.50	16.69	19.04
CaO	0.23	0.27	0.20	0.19
Na_2O	2.09	2.27	0.42	0.54
K_2O	0.00	0.01	0.01	0.00
V_2O_3	0.03	0.06	0.11	0.03
Cr_2O_3	0.04	0.00	0.08	0.00
NiO	0.00	0.00	0.04	0.02
ZnO	n.d.	n.d.	n.d.	n.d.
Total	92.32	92.25	98.32	97.34
Number of cations based on 22 oxygens				
Si	5.6184	5.6534	7.2455	7.2355
Ti	0.0508	0.0326	0.0108	0.0084
Al	2.9541	2.8002	0.7833	0.7899
Fe	2.2604	2.1742	2.7145	2.2947
Mn	0.0114	0.0112	0.0248	0.0160
Mg	3.6089	3.8629	3.4495	3.9094
Ca	0.0372	0.0428	0.0299	0.0282
Na	0.6013	0.6516	0.1137	0.1453
K	0.0006	0.0017	0.0014	0.0009
V	0.0036	0.0067	0.0127	0.0028
Cr	0.0041	0.0000	0.0086	0.0000
Ni	0.0000	0.0000	0.0042	0.0019
Zn	n.d.	n.d.	n.d.	n.d.

Table 15. Spinel analyses. i/c = inclusion in cordierite, i/g = inclusion in garnet. The other spinels analysed have the assemblage spl-opx-pl-Fe ox.

Code	19a—i/c	62—i/g	52b—i/g	52	54b	61
SiO_2	0.03	0.01	0.23	0.02	0.03	0.02
TiO_2	0.02	0.00	0.09	0.09	0.02	0.00
Al_2O_3	57.71	61.30	62.10	60.29	59.47	59.43
FeO	26.82	26.33	25.90	29.99	25.52	16.89
MnO	0.05	0.01	0.00	0.00	0.37	0.33
MgO	5.70	7.72	12.10	8.10	5.19	4.35
CaO	0.01	0.01	0.00	0.01	0.01	0.00
Na_2O	0.19	0.08	n.d.	0.02	0.31	0.71
K_2O	0.00	0.00	n.d.	0.01	0.04	0.00
V_2O_3	0.70	0.13	n.d.	0.05	0.01	0.02
Cr_2O_3	2.32	0.26	0.00	0.01	0.03	0.02
NiO	0.04	0.07	n.d.	0.02	0.00	0.00
ZnO	6.10	3.26	0.50	0.41	9.10	20.22
Total	99.70	99.17	100.92	99.02	100.10	102.00
Number of cations based on 4 oxygens						
Si	0.0007	0.0004	0.0061	0.0005	0.0008	0.0005
Ti	0.0005	0.0000	0.0018	0.0020	0.0004	0.0000
Al	1.9240	1.9939	1.9460	1.9691	1.9783	1.9778
Fe	0.6344	0.6076	0.5759	0.6950	0.6024	0.3987
Mn	0.0012	0.0002	0.0000	0.0000	0.0088	0.0080
Mg	0.2402	0.3175	0.4795	0.3345	0.2184	0.1831
Ca	0.0005	0.0002	0.0000	0.0002	0.0002	0.0000
Na	0.0105	0.0044	n.d.	0.0010	0.0167	0.0391
K	0.0000	0.0000	n.d.	0.0005	0.0014	0.0000
V	0.0159	0.0029	n.d.	0.0012	0.0003	0.0004
Cr	0.0519	0.0057	0.0000	0.0002	0.0006	0.0004
Ni	0.0008	0.0015	n.d.	0.0005	0.0001	0.0001
Zn	0.1275	0.0663	0.0098	0.0084	0.1897	0.4215

Table 16. Iron oxide analyses and the magnetite-ilmenite temperatures according to Spencer & Lindsley (1981). c = core, r = rim of grain. Fe_2O_3 calculated from the analysis according to Carmichael (1967).

	Ilmenites				Magnetites			
Code	20a—c	20a—r	59a—c	59a—r	20a—c	20a—r	59a—c	59a—r
TiO_2	50.00	51.20	46.60	46.20	0.03	0.44	0.07	0.10
FeO	45.58	45.94	44.65	44.35	30.58	31.76	31.08	30.30
Fe_2O_3	4.25	2.63	6.61	6.95	67.97	68.87	68.96	68.72
MnO	0.03	0.04	0.19	0.12	0.00	0.00	0.00	0.09
MgO	0.71	0.70	0.02	0.11	0.02	0.00	0.03	0.39
Total	100.57	100.50	98.08	97.73	98.59	101.08	100.14	99.60
Number of cations based on 3 oxygens					Number of cations based on 4 oxygens			
Ti	0.9464	0.9669	0.9135	0.9088	0.0009	0.0126	0.0020	0.0029
Fe_2	0.9593	0.9647	0.9734	0.9702	0.9993	1.0122	0.9999	0.9771
Fe_3	0.0805	0.0497	0.1297	0.1367	1.9985	1.9751	1.9962	1.9945
Mn	0.0006	0.0009	0.0042	0.0027	0.0000	0.0000	0.0000	0.0029
Mg	0.0266	0.0262	0.0008	0.0043	0.0012	0.0000	0.0017	0.0224
T°C	428	487	495	484				

Table 17. The grt-opx-temperatures and pressures and the grt-opx-pl-qtz-pressures. T_1 = according to Harley (1984a); T_2 = according to Perchuk et al. (1985); T_3 = according to Sen and Bhattacharya (1984); P_1 = P-Mg, P_2 = P-Fe according to Perkins and Chipera (1985); P_3 = according to Newton and Perkins (1982); P_4 = according to Harley (1984b). An asterisk after the code implies that plagioclase is absent from the assemblage. Sample 58a** is from mangerite near the contact.

Code	$X_{Ca}Pl$	$X_{Ca}Grt$	$X_{Mg}Grt$	$X_{Fe}Grt$	$X_{Fe}Opx$	$a_{En}Opx$	$a_{Fs}Opx$	$X_{Al}Opx$	T_1	T_2	T_3	P_1	P_2	P_3	P_4
Cores of large grains															
52c	0.343	0.031	0.336	0.591	0.430	0.286	0.129	0.142	799	774	912	4.3	5.9	5.4	5.5
52a	0.216	0.031	0.356	0.603	0.452	0.254	0.153	0.166	883	834	1050	7.4	8.5	8.7	6.0
54a	0.177	0.018	0.325	0.612	0.410	0.295	0.122	0.158	695	665	755	4.4	5.9	5.7	2.3
53	0.322	0.043	0.279	0.642	0.479	0.251	0.204	0.058	804	821	920	5.4	5.8	5.8	12.2
61	0.276	0.037	0.270	0.605	0.455	0.256	0.171	0.106	723	743	801	5.2	5.2	5.4	5.2
18	0.374	0.030	0.329	0.628	0.455	0.255	0.178	0.116	825	805	955	4.0	4.8	5.3	7.5
55d	0.328	0.032	0.323	0.619	0.477	0.237	0.184	0.128	879	850	1043	5.2	5.9	6.3	7.7
Orthopyroxene altered to garnet															
52	0.210	0.018	0.320	0.650	0.445	0.262	0.160	0.151	737	711	822	3.8	4.9	5.1	3.3
54	0.183	0.018	0.310	0.617	0.420	0.281	0.132	0.163	685	659	742	4.2	5.3	5.1	1.7
55	0.308	0.026	0.330	0.622	0.464	0.249	0.176	0.128	852	818	998	4.4	5.4	5.5	7.3
55a	0.296	0.026	0.320	0.629	0.485	0.237	0.166	0.135	881	845	1050	4.7	6.0	5.9	7.3
55b	0.308	0.025	0.296	0.655	0.468	0.252	0.160	0.133	751	741	845	3.3	4.5	4.2	4.1
55c	0.293	0.037	0.280	0.658	0.380	0.359	0.135	0.025	614	618	641	3.3	4.8	4.2	13.8
Garnet altered to orthopyroxene															
52b	0.230	0.020	0.322	0.650	0.406	0.312	0.125	0.135	658	646	704	3.0	4.8	4.5	2.6
52d	0.326	0.028	0.313	0.613	0.385	0.340	0.111	0.115	641	637	678	2.8	4.5	3.5	3.5
52c	0.213	0.019	0.339	0.633	0.383	0.336	0.112	0.133	652	630	693	3.2	5.2	4.7	2.9
54b	0.187	0.019	0.281	0.640	0.418	0.291	0.125	0.144	614	613	645	3.6	4.6	4.2	0.7
54c*	0.177	0.019	0.332	0.609	0.392	0.323	0.112	0.139	677	651	728				3.1
Contact zones of mangerites															
63—45m.	0.360	0.045	0.177	0.716	0.540	0.193	0.266	0.026	647	718	699	3.8	2.8	2.9	11.6
56—3m.	0.316	0.031	0.243	0.708	0.532	0.197	0.255	0.084	754	787	855	3.9	3.5	4.3	6.8
57a—100m.	0.334	0.031	0.287	0.656	0.457	0.264	0.187	0.085	728	742	808	3.5	4.1	4.5	7.3
57—100m.	0.348	0.032	0.300	0.643	0.469	0.256	0.187	0.085	801	801	916	4.0	4.8	4.9	9.2
57b—100m.	0.350	0.040	0.257	0.676	0.468	0.262	0.178	0.086	671	716	729	3.8	4.2	4.3	5.2
64—160m.	0.359	0.034	0.286	0.658	0.449	0.276	0.167	0.094	700	722	767	3.4	4.2	4.3	5.7
58a**	0.354	0.040	0.206	0.728	0.593	0.155	0.303	0.060	805	852	936	4.8	3.8	4.5	9.6
58—2m.	0.340	0.038	0.243	0.692	0.506	0.222	0.212	0.086	707	754	784	4.0	4.0	4.4	5.5
59a—200m.	0.253	0.030	0.218	0.706	0.537	0.193	0.226	0.105	686	739	757	4.3	3.8	4.4	2.5
— orthopyroxene altered to garnet															
59e—200m.	0.255	0.031	0.204	0.721	0.529	0.202	0.219	0.100	625	693	671	3.8	3.2	3.7	1.6
59d—200m.	0.247	0.032	0.188	0.729	0.507	0.232	0.215	0.054	569	646	593	3.3	2.7	3.0	4.8
59c—200m.	0.272	0.028	0.220	0.702	0.500	0.226	0.217	0.080	633	685	678	3.2	2.8	3.3	4.1
— garnet altered to orthopyroxene															
59b—200m.	0.251	0.031	0.190	0.736	0.501	0.234	0.208	0.068	551	628	570	3.1	2.5	2.7	2.6

The third group contains the results based on the analytical data on points close to the garnet rim and the compositions of the orthopyroxene-plagioclase coronas formed as alteration products of garnet ($T = 613—677°C$, $P = 4 \pm 0.8$ kb). Orthopyroxene coronas such as these are clearly richer in Mg than are the large primary grains, which may imply that their composition was totally changed by later diffusion. Should this be the case, then the P-Mg (P_1 in Table 17) calculated according to Perkins and Chipera (1985) is too low for the time of formation, as the ln K of the Mg reaction increases when the Mg in orthopyroxene is increased by diffusion. Accordingly, the differences between P-Mg and P-Fe pressure values are highest, averaging 1.63 kb, in this group. When based on the compositions of the cores of the large grains, the differences average 0.87 kb, and are 0.59 kb in the mangerite contacts.

According to Ellis and Green (1985), reaction coronas may form below the blocking temperatures of the cation exchange reactions. If this is what happened, then weak zoning in the pyroxene corona, on garnet, may suggest that the corona was formed at temperatures below the blocking temperature of the cation exchange reaction. Figure 17b shows, however, that after the formation of the garnet corona, diffusion took place between orthopyroxene and garnet.

The fourth group comprises the analyses based on the compositions of the cores of the grains in the samples that were taken no farther than 200 m from the contacts of the mangerite intrusions. The pressures are distinctly lower than in the first and second groups on average ($P = 4 \pm 0.5$ kb, $T = 647—801°C$), but almost equal to those in the third group. Analyses 63—45m, 56—3m and 64—160m, are from the Lampaanjärvi block (II). The orthopyroxenes of this group are conspicuously richer in iron and poorer in aluminium than elsewhere.

Determinations 59c—200m, 59d—200m, and 59c—200m, were based on the compositions of orthopyroxene and the garnet corona on it; 59b—200m was calculated from the compositions of the margins of garnet (but not of the outermost rim) and the surrounding orthopyroxene corona. The pressures and temperatures given by these determinations are the lowest recorded block from the granulite because of the high Fe content of the phases.

Ilmenite and plagioclase inclusions in garnet

Garnet 52b, which is a large grain 20 mm in diameter, contains abundant plagioclase, magnetite and ilmenite inclusions and some spinel inclusions. Figs 19 and 17a illustrate the zoning of this garnet grain. The Mg content first declines from the core towards the rim, and then increases slightly before declining steeply in the rim. The profile in Fig. 19 shows two other zones that are richer in Ca than the environment. The anorthite content of the plagioclase inclusions increases with the increase in the grossular component. The manganese content of the ilmenite inclusions first declines from the garnet core towards the rim, then rises and finally declines again. However, the ilmenite right at the edge of the garnet is fairly rich in manganese relative to the other ilmenites. This case excluded, the manganese content of ilmenite shows a slight positive correlation with the pyrope content of garnet (Fig. 20).

Pressure and temperature were calculated using the grt-rt-ilm-pl-qtz barometer, GRIPS (Bohlen and Liotta, 1986) and the thermometer based on the partition of iron and manganese between garnet and ilmenite (Pownceby *et al.*, 1987). Since the garnet is free from rutile inclusions the pressure values represent maximum ones. The manganese contents of garnet and ilmenite are very low, and hence the temperatures can be considered merely indicative. Ilmenite is invariably intergrown with magnetite, and the ilmenite-

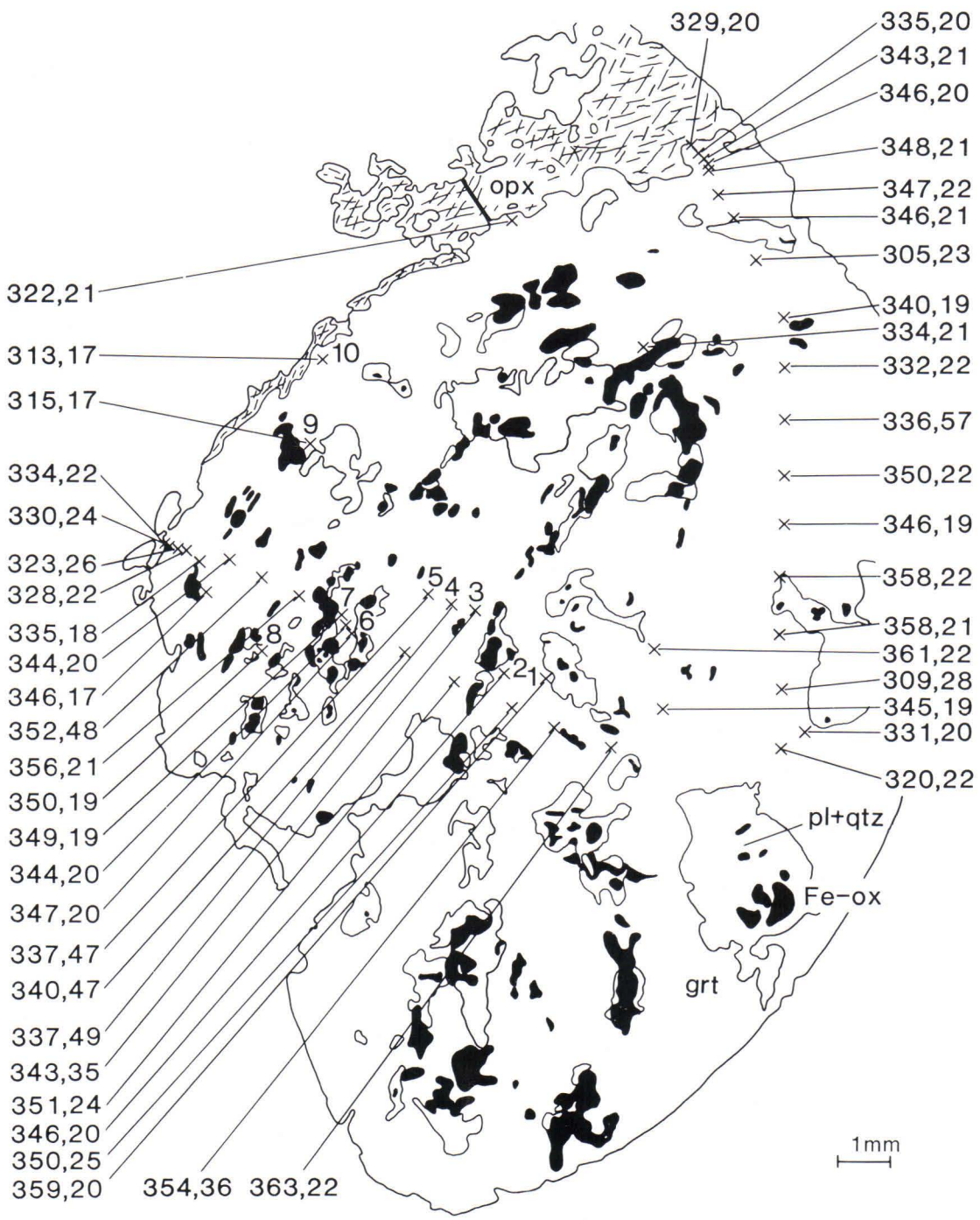

Fig. 19. Composition distribution in garnet 52b. Numbers referring to crosses are X_{Mg} and $X_{Ca} \times 1000$. The numbers on the right side of the crosses refer to the points that are used in the calculations presented in Table 18. The line across opx refers to the zoning profile in Fig. 16.

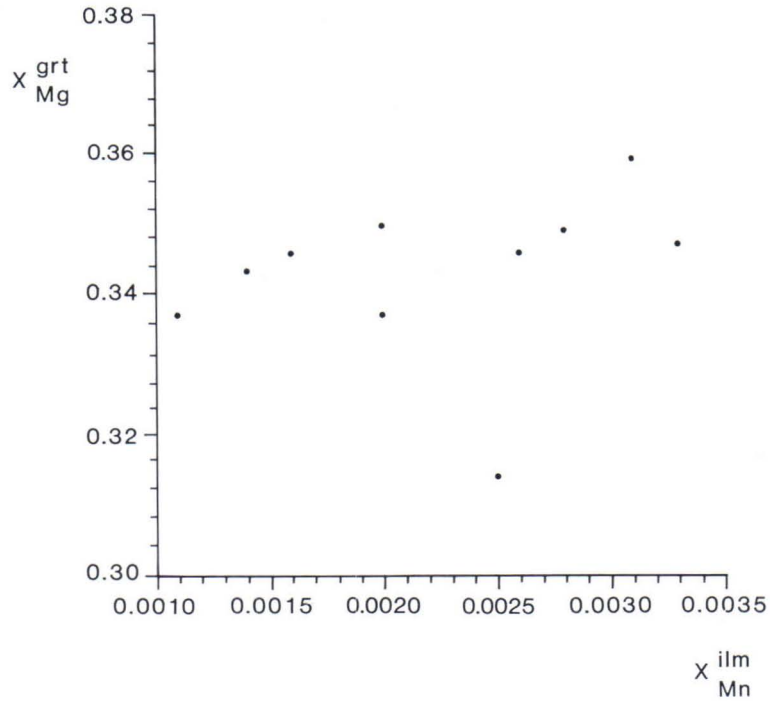

Fig. 20. The correlation between the X_{Mg} of garnet 52b and the X_{Mn} of its ilmenite inclusions.

magnetite thermometer implies equilibration at low temperatures. This has affected the iron content of ilmenite and the grt-ilm partition coefficient. The manganese content of garnet is fairly constant ($X_{Mn} = 0.008—0.010$); consequently, the calculated temperature is predominantly a function of the manganese content of ilmenite. The magnetite in contact with ilmenite contains very little manganese or none at all.

The thermometer shows a temperature that first falls, then rises and finally falls again from the core of the grain towards the rim. The ln K

Table 18. The GRIPS-pressures (Bohlen and Liotta 1986) and the garnet-ilmenite temperatures (Pownceby et al. 1987, equation 13) for the inclusions in garnet 52b. The activities of almandine and grossular were calculated according to Ganguly and Saxena (1984) and the activity of anorthite according to Newton (1983). Ilmenite is treated as an ideal solution. Numbers after the code refer to the Fig. 19.

Code	X_{Ca}Pl	X_{Fe}Grt	X_{Mn}Grt	X_{mg}Grt	X_{Ca}Grt	X_{Fe}Ilm	X_{Mn}Ilm	lnK (GRIPS)	P kb	T°C
52b-1	0.251	0.612	0.009	0.359	0.020	0.9194	0.0031	10.43158	5.7	742
52b-2	0.243	0.625	0.010	0.346	0.020	0.906	0.0026	10.44287	4.8	640
52b-3	0.392	0.613	0.009	0.343	0.035	0.9346	0.0014	10.87951	3.2	474
52b-4	0.427	0.603	0.011	0.337	0.049	0.9335	0.0020	9.97109	4.2	515
52b-5	0.433	0.606	0.010	0.337	0.047	0.9403	0.0011	10.27102	3.0	395
52b-6	0.213	0.624	0.009	0.347	0.020	0.9593	0.0033	10.12981	6.2	766
52b-7	0.237	0.623	0.009	0.349	0.019	0.9552	0.0028	10.68684	5.2	698
52b-8	0.259	0.623	0.008	0.350	0.019	0.9544	0.0020	11.26502	4.0	615
52b-9	0.226	0.629	0.009	0.346	0.017	0.9512	0.0016	11.40417	3.1	514
52b-10	0.222	0.661	0.009	0.313	0.017	0.9561	0.0025	10.98800	4.6	679

of the GRIPS reaction first declines from c. 10.4 in the core to c. 9.9 in the calcium-rich zone, and then increases to c. 11.3 close to the rim (Table 18). If the temperatures given by the thermometer refer to the growth of the grain, this implies that cooling was initially almost isobaric, but then pressure increased slightly with the increase in temperature and the final cooling was with a small drop in pressure. According to the GRIPS barometer, the grains grew at 4—6 kb pressure, assuming that the lowest temperatures derived from the grt-ilm thermometer are too low.

Age determinations

U-Pb age determinations on zircon and titanite were made at the Isotope Laboratory of the Geological Survey of Finland from a gneissose quartz diorite from Mustikkamäki, which is located at the eastern margin of the granulite block (III) next to a fault. The mineral assemblage is hbl-bt-cpx-pl-qtz-ilm-ttn-ap-zr ± opx. The rock is strongly retrograde; diopside has always altered to hornblende and hornblende to biotite. Titanite occurs frequently as coronas on ilmenite. There are two zircon populations, long gemlike needles and stumpy ones, whose ages are between 1895 and 1915 Ma. There are also two sorts of sphenes, light and dark brown, whose ages are 1855—1864 Ma.

Data on the two zircon fractions consisting of long needle-like crystals (A, C) having L/B ratios of 7 or more and on two fractions of stumpy zircons ((B, D; L/B 2—3) are plotted on the U-Pb concordia diagram (Fig. 21). The U-Pb data

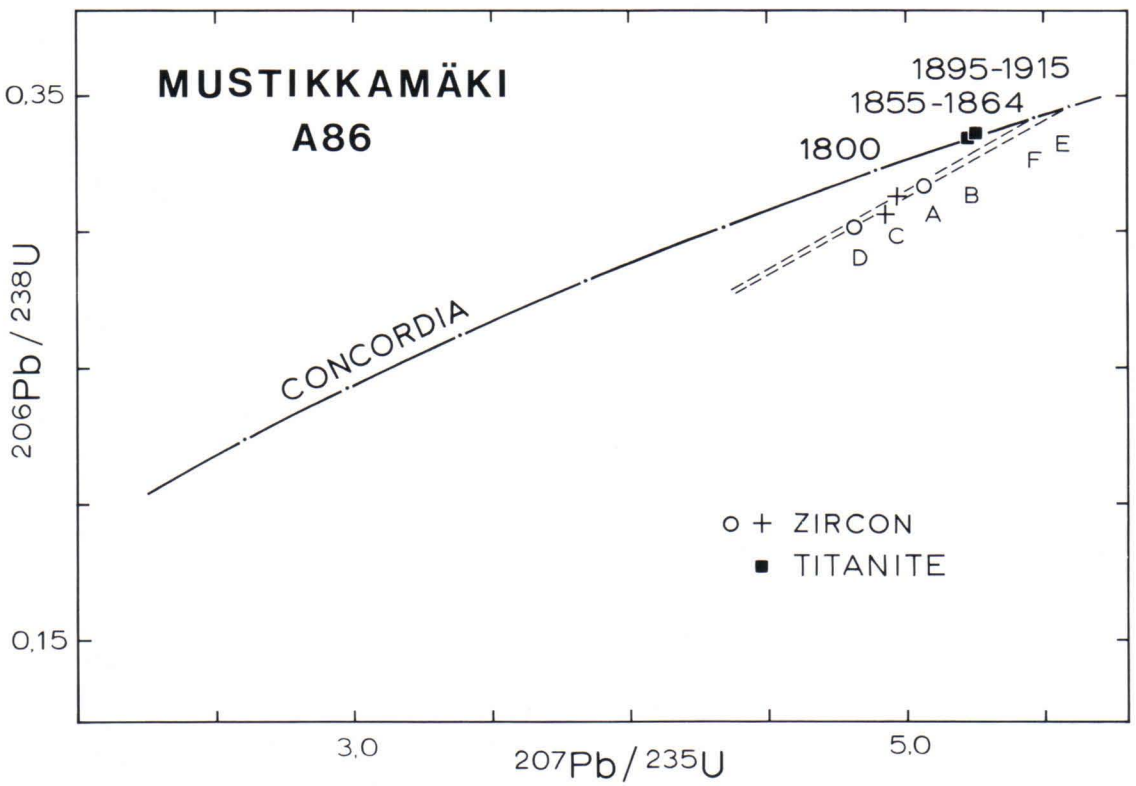

Fig. 21. U-Pb concordia diagram for zircons and for titanites from the Mustikkamäki pyroxene quartz-diorite, Pielavesi. Crosses mark the long zircon crystals, circles mark the short, stumpy zircons. Letters refer to the analytical data in table 19. Fraction C (weight 0.7 mg) includes close to 3 % uncertainty.

on four fractions define an ambiguous discordance pattern, the chord to which would give an upper intercept with concordia at 1890 ± 77 Ma (2 sigma). This resultant chord does not, however, have real age significance, because, except for fraction A, the 207Pb/206Pb ages of moderately discordant age patterns are higher than 1890 Ma. Fraction C (0.7 mg) can be ignored because of the large uncertainty due to the 206Pb/204Pb ratio. The age limits on the concordia diagram define the continuous diffusion trajectories through fractions A and D.

For present purposes, the important point is the age difference between zircon and titanite. The titanite fractions differ in content of uranium and common lead as can be seen in Table 19. The dark brown titanite crystals (F) picked by hand from density fraction 3.3—3.4 g/cm^3 are fairly rich in uranium (194 µg/g) and in common lead (206Pb/204Pb 442).

The heavier fraction, E, is quite clean of common lead (6/4 = 1214) and has uranium only 33 µg/g. This fraction consists of light brown titanite mixed with one quarter of dark brown crystals.

PTt evolution

The results from the studies of the metamorphic reactions and thermobarometry can be summarized by stating that metamorphism culminated in the Pielavesi granulite block at a pressure of about 5.5 kb and at a temperature of 800—880°C. This stage was reached during the first or second deformation event, as implied by the mineral growth associated with the early deformation thoughout the area (Pajunen, 1986 and 1988; Ward, 1988). The poikiloblastic areas in the cores of the garnet grains (Fig. 7) may indicate that crystallization was rapid at the onset of crystal growth, but that later it was more equilibrated, resulting in the formation of a solid grain margin.

The culmination was followed by isobaric cooling (Fig. 22), during which the net transfer reactions produced garnet coronas.

The information obtained from the zoning and the inclusions in garnet 52b is indicative of a second thermal pulse. This concept is supported by the zoning of many garnets, with the Mg contents increasing close to the rim.

Some ages on the gneissose granitoids of the craton margin are indicative of orogenic events about 1920—1930 Ma ago (Helovuori, 1979; Korsman *et al.*, 1984). At Laajamäki in the Pielavesi block an intensely deformed gneiss granite has also been dated with the U-Pb of zircon at 1920 Ma (Vaasjoki & Sakko, 1988). However, the zircon from the garnet-cordierite-orthopyroxene rock at Sahinperä gives an age of 1889 ± 3 Ma (Vaasjoki & Sakko, op.cit.), which probably refers to metamorphism. Within error limits, the age is the same as that of the mangerite intrusion at Vaaraslahti, 1884 ± 5 Ma (Salli, 1983). The U-Pb age on zircon from the high-grade thermal aureole of the Vaaraslahti intrusion in 1892 ± 5 Ma (Vaasjoki and Sakko op.cit.).

So the evolution of the granulite facies metamorphism in the Pielavesi block may be caused by two successive magmatic pulses with a cooling period between them.

The pressure was, however, lower in the contact zones of the mangerite intrusions than elsewhere in the area. It is conceivable that the large intrusions retained their heat for a long time, and so crystallization took place at the contacts when the crust had already been slightly uplifted. The alternative is that the PT path advanced anticlockwise during the contact metamorphic heating as crystallization took place at the contacts earlier and at lower pressure. The large poikiloblastic garnet grains rich in quartz inclusions and

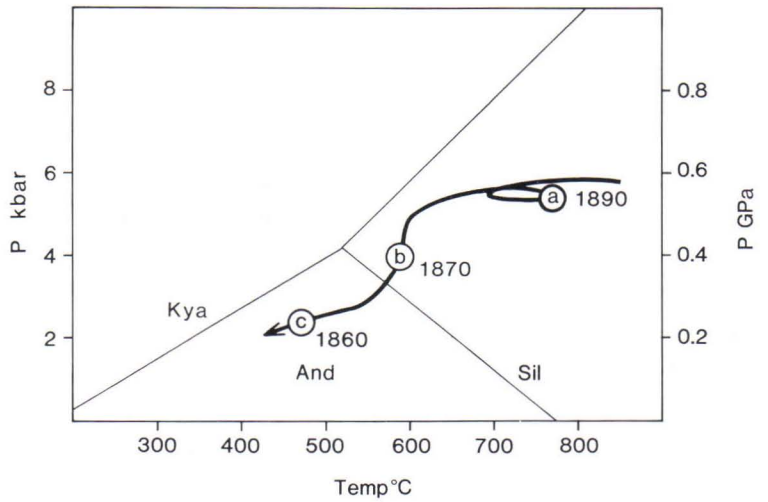

Fig. 22. The possible PTt path of the Pielavesi granulite zone. a = U-Pb age of zircon, b = U-Pb age of monazite, C = U-Pb age of sphene.

Table 19. U-Pb analytical data for zircons and titanites from the pyroxene quartz diorite, Mustikkamäki, Pielavesi.

Sample no.	Fraction (g/cm^3) Ø = grain size, µm	Concentration µg/g		$\frac{206_{Pb}}{204_{Pb}}$ measured	Isotopic composition of lead $206_{Pb} = 100$			Atom ratios and radiometric ages, Mo		
		238_U	206_{Pb}		204	207	208	$\frac{206_{Pb}}{238_U}$	$\frac{207_{Pb}}{235_U}$	$\frac{207_{Pb}}{206_{Pb}}$
A86-Mustikkamäki, Pielavesi; pyroxene quartz-diorite										
A86A	4.3<d<4.45 long crystals	448.3	121.33	18437	.000092	11.520	7.468	.3128 ±18 1754	4.968 ±31 1813	.11519 ±17 1883
B	4.3<d<4.45 stumpy	456.1	124.98	23481	.001980	11.622	5.866	.3167 ±23 1773	5.063 ±38 1829	.11595 ±11 1894
C	4.2<d<4.3 long crystals	576.6	152.60	585	.15138	13.723	23.996	.3059 ±28 1720	4.93 ±16 1806	.1168 ±32 1908
D	4.2<d<4.3 stumpy	699.2	182.32	1566	.06044	12.399	7.431	.3013 ±38 1697	4.812 ±62 1787	.11582 ±23 1892
E	titanite 3.5<d<3.6	32.98	9.57	1214	.07639	12.435	6.398	.3354 ±21 1864	5.272 ±37 1864	.11400 ±27 1864
F	titanite 3.3<d<3.4 dark brown	193.7	55.98	442	.22295	14.367	11.897	.3340 ±30 1857	5.225 ±50 1856	.11346 ±30 1855

$238_U = 1.55125 \times 10^{-10}/a$
$235_U = 9.8485 \times 10^{-10}/a$
atomic ratio: $238_U/235_U = 137.88$

the sector-twinned cordierite in the vicinity of the mangerites are indicative of rapid crystallization during contact metamorphism. In that case the mineral compositions would not have been re-equilibrated in the contact zone even though the thermal effect of the intrusions extended rather far, for example, in block II (Fig. 1), and crystallization was more equilibrated farther from the contacts.

The pressures given by the orthopyroxene coronas (Table 17) are similar to those in the contact zones of the mangerites, about 4.5 kb; so the corona formation may be connected with the contact metamorphic heating. On the other hand, the zoning and inclusions, e.g. in garnet 52 b (Fig. 19), show evidence of cooling and heating during the garnet growth the orthopyroxene corona formation being the last textural event; so it probably denotes the beginning of block uplift.

During the final stage, intense rehydration reactions took place, altering cordierite into biotite and sillimanite or andalusite, and orthopyroxene into orthoamphibole. Alterations of this kind are visible both within and outside the contact aureoles. The garnet-biotite intergrowths are also related to the later cooling stage, as is the equilibration of the magnetite-ilmenite pair. The mag-ilm temperatures calculated according to Spencer and Lindsley (1982) for the granulite area are less than 500°C (Table 16). The U-Pb age on monazite at Sahinperä is 1873 ± 5 Ma, and refers to cooling down to about 500—600°C (Vaasjoki & Sakko, 1988). According to Mattinson (1982), the U-Pb system in titanite appears to close at ca. 450—500°C. Titanite ages from Mustikkamäki show that these temperatures were achieved ca. 1860 Ma ago. The K-Ar ages of biotite are 1770—1790 Ma in the granulite zone (Haudenschild, 1988).

DISCUSSION

The crystallization history of rocks is related to macrotectonic processes in the area, as theoretically demonstrated by Thompson and England (1984). The reactions between minerals in the tectonically thickened parts of the crust reflect an isothermal drop in pressure near the metamorphic culmination, as shown by studies undertaken in the Alps and Caledonides (Droop and Bucher-Nurminen, 1984; Selverstone *et al.*, 1984; Johansson and Möller, 1986). On the other hand, there are numerous cases, mainly in Precambrian granulite areas (Sandiford and Powell, 1986), in which the maximum temperature was followed by isobaric cooling. Isobaric cooling has been associated with extension of the crust (Sandiford and Powell, op.cit.), magmatic thickening of the crust (in which case the PT path is anticlockwise, Bohlen, 1987) or, in the case of tectonically thickened crust, with the PT history of the rocks buried at the greatest depth, at which, once isostatic equilibrium was attained, cooling continued isobarically (Ellis, 1987).

According to Bohlen (op. cit.), typical features of many granulites are: a maximum temperature of c. 800°C at c. 7.5 ± 1 kb pressure; temperature rather than pressure differences in relation to the surrounding rocks of the amphibolite facies; almost isobaric cooling following the culmination of metamorphism; and coarse-grained sillimanite. Bohlen attributes these features to magmatic thickening of the crust, as the temperature maximum is reached before the pressure maximum and the rocks remain in the sillimanite field for a long period during their crystallization history. Broadly speaking, these specifications describe the Pielavesi granulite area, too. True, the coarse-grained sillimanite is rare, but then sillimanite is predominantly a retrograde

mineral; therefore, cooling started in the sillimanite field.

In the light of age determinations and detailed petrography and thermobarometry, it would appear that two strong thermal pulses were effective in the area, of which the latter, which took place 1890 Ma ago, was associated with tensional magmatism, as maintained by Marttila (1976) and Korsman *et al.* (1984).

As stated by Korsman *et al.* (1988), the evolution of the southern part of the Svecofennides differs in many aspects, e.g. temporally, from the northern part. Study of the cooling history of the Pielavesi granulite area shows that near the Archaean craton margin the high-grade rocks were already relatively cold 1860 Ma ago, whereas the granulites in southern Finland reached the thermal maximum 1830—1810 Ma BP (Korsman *et al.* 1984).

ACKNOWLEDGEMENTS

Dr. Kalevi Korsman, Prof. Heikki Papunen and Dr. Neil Hudson read the manuscript and made comments which greatly improved it. Mr. Bo Johanson made the microprobe analyses at the Geological Survey and Mr. Seppo Sivonen was responsible for the analyses at Oulu University. Mr. Väinö Hoffrén made the whole-rock analyses. The figures were drawn by Mrs. Ritva Forsman, Mrs. Elsa Järvimäki and Miss Liisa Sirén. Discussions with Dr. Kalevi Korsman, Dr. Matti Vaasjoki and Mr. Matti Pajunen were of great help during the work. The manuscript was translated into English by Mrs. Gillian Häkli. To all these persons I express my cordial thanks.

REFERENCES

Aranovich, L.Ya. & Podlesskii, K.K. 1983. The cordierite-garnet-sillimanite-quartz equilibrium: experiments and applications. *In* Kinetics and Equilibrium in Mineral Reactions *ed. by* S.K. Saxena. Advances in Physical Geochemistry 3, 173—198. Springer-Verlag, New York.

Bohlen, S.R. 1987. Pressure-temperature-time paths and a tectonic model for the evolution of granulites. Journal of Geology 95, 617—632.

Bohlen, S.R. & Liotta, J.J. 1986. A barometer for garnet amphibolites and garnet granulites. Journal of Petrology 27, 1025—1034.

Bohlen, S.R. & Lindsley, D.H. 1987. Thermometry and barometry of igneous and metamorphic rocks. Ann. Rev. Earth Plan. Sci. 15, 397—420.

Carmichael, I.S.E. 1967. The iron-titanium oxides of salic volcanic rocks and their associated ferromagnesian silicates. Contrib. Mineral. Petrol. 14, 36—64.

Droop, G.T.R. & Bucher-Nurminen, K. 1984. Reaction textures and metamorphic evolution of sapphirine-bearing granulites from the Gruf Complex, Italian Central Alps. J. Petrol 25, 766—803.

Edwards, R.L. & Essene, E.J. 1988. Pressure, temperature and C-O-H fluid fugacities across the amphibolite-granulite transition, Northwest Adirondack Mountains, New York. J. Petrol. 29, 39—72.

Ellis, D.J. 1980. Osumilite-sapphirine-quartz granulites from Enderby Land, Antarctica: P-T conditions of metamorphism, implications for garnet-cordierite equilibria and the evolution of the deep crust. Contrib. Mineral. Petrol. 74, 201—210.

Ellis, D.J. 1987. Origin and evolution of granulites in normal and thickened crust. Geology 15, 167—170.

Ellis, D.J. & Green, D.H. 1985. Garnet-forming reactions in mafic granulites from Enderby Land, Antarctica — implications for geothermometry and geobarometry. J. Petrol. 26, 633—662.

Ferry, J.M. & Spear, F.S. 1978. Experimental calibration of the partitioning of Fe and Mg between biotite and garnet. Contrib. Mineral. Petrol. 66, 113—117.

Ganguly, J. & Kennedy, G.C. 1974. The energetics of natural garnet solid solution. I. Mixing of the aluminosilicate end members. Contrib. Miner. Petrol. 48, 137—148.

Ganguly, J. & Saxena, S.K. 1984. Mixing properties of aluminosilicate garnets: constraints from natural and experimental data, and applications to geothermobarometry. Am. Mineral. 69, 88—97.

Ghent, E.M. & Stout, M.Z. 1981. Geobarometry and geothermometry of plagioclase-biotite-garnet-muscovite assemblages. Contrib. Mineral. Petrol. 76, 92—97.

Grad, M. & Luosto, U. 1987. Seismic models of the crust of the Baltic shield along the SVEKA profile in Finland. Ann. Geophys. 5B, (6), 639—650.

Harley, S.L. 1984a. An experimental study of the partitioning of Fe and Mg between garnet and orthopyroxene. Contrib. Mineral. Petrol. 86, 359—373.

Harley, S.L. 1984b. The solubility of alumina on orthopyroxene coexisting with garnet in FeO-MgO-Al_2O_3-SiO_2 and CaO-FeO-MgO-Al_2O_3-SiO_2. J. Petrol. 25, 665—696.

Harley, S.L. 1985. Garnet-orthopyroxene bearing granulites from Enderby Land, Antarctica: Metamorphic pressure-temperature-time evolution of the Archaean Napier complex. J. Petrol. 26/4, 819—856.

Harley, S.L. 1986. A sapphirine-cordierite-garnet-sillimanite granulite from Enderby Land, Antarctica: implications for FMAS petrogenetic grids in the granulite facies. Contrib. Mineral. Petrol. 94, 452—460.

Harris, N.B.W. & Holland, T.J.B. 1984. The significance of cordierite-hypersthene assemblages from the Beitbridge region of the Central Limpopo Belt; evidence for the rapid decompression in the Archaean? Am. Mineral. 69, 1036—1049.

Haudenschild, V. 1988. K-Ar age determination on biotite and muscovite in the Pihtipudas—Iisalmi and Joroinen areas in eastern Finland. Geol. Surv. Finland, Bull 343, 33—50.

Helovuori, O. 1979. Geology of the Pyhäsalmi ore deposit, Finland. Econ. Geol. 74, 1084—1101.

Hodges, K.V. & Spear, F.S. 1982. Geothermometry, geobarometry and the Al_2SiO_5 triple point at Mt. Moosilauke, New Hampshire. Am. Mineral. 67, 1118—1134.

Hodges, K.V. & Crowley, P.D. 1985. Errors estimation and empirical geothermobarometry for pelitic systems. Am. Mineral. 70, 702—709.

Holdaway, M.J. & Lee, S.M. 1977. Fe-Mg cordierite stability in high grade pelitic rocks based on experimental, theoretical and natural observations. Contrib. Mineral. Petrol. 63, 175—198.

Hölttä, P. 1986. Observations on the metamorphic reactions and PT conditions in the Turku granulite area. Geol. Surv. Finland Bull. 339, 43—58.

Hudson, N.F.C. 1985. Conditions of Dalradian metamorphism in the Buchan area, NE Scotland. J. Geol. Soc. London 142, 63—76.

Huhtala, T. 1979. The geology and zinc-copper deposits of the Pyhäsalmi-Pielavesi district, Finland. Econ. Geol. 74, 1069—1083.

Hutcheon, I., Froese, E. & Gordon, T.M. 1974. The assemblage quartz-sillimanite-garnet-cordierite as an indicator of metamorphic conditions in the Daly Bay Complex, N.W.T. Contrib. Mineral. Petrol. 44, 29—34.

Indares, A. & Martignole, J. 1985. Biotite-garnet geothermometry in the granulite facies: the influence of Ti and in biotite. Am. Mineral. 70, 272—278.

Jansen, J.B.H., Blok, R.J.P., Bos, A. & Scheelings, M. 1985. Geothermometry and geobarometry in Rogaland and preliminary results from the Bamble area, South Norway. *In* The Deep Proterozoic Crust in the North Atlantic Provinces ed. by Tobi, A.C. and Touret, J.L.R. NATO ASI Series C: Mathem. Phys. Sci. 158, 499—516. D. Reidel Publ. Comp.

Johansson, L. & Möller, C. 1986. Formation of sapphirine during retrogression of a basic high-pressure granulite, Roan, Western Gneiss Region, Norway. Contrib. Mineral. Petrol. 94, 29—41.

Korsman, K. 1977. Progressive metamorphism of the metapelites in the Rantasalmi—Sulkava area, southeastern Finland. Geol. Surv. Finland Bull. 290, 82 p.

Korsman, K., Hölttä, P., Hautala, T. & Wasenius, P. 1984. Metamorphism as an indicator of evolution and structure of the crust in Eastern Finland. Geol. Surv. Finland Bull. 328, 40 p.

Korsman, K. & Kilpeläinen, T. 1986. Relationship between zonal metamorphism and deformation in the Rantasalmi—Sulkava area, southeastern Finland. Geol. Surv. Finland Bull. 339, 33—42.

Korsman, K., Niemelä, R. & Wasenius, P. 1988. Multistage evolution of the Proterozoic crust in the Savo schist belt, eastern Finland, Geol. Surv. Finland Bull. 343, 89—96.

Kretz, R. 1983. Symbols for rock-forming minerals. Am. Mineral. 68, 277—279.

Kuosmanen, V. (ed.) in press. Exploration target selection by integration of geodata using statistical and image processing techniques: an example from central Finland. Atlas. Geological Survey of Finland, Rep. Invest.

Luosto, U., Lanne, E., Korhonen, H., Guterch, A., Grad, M., Materzok, R. & Perchuc, E. 1984. Deep structure of the Earth's crust on the SVEKA profile in central Finland. Ann. Geophys. 2 (5), 559—570.

Martignole, J. Sisi, J.C. 1981. Cordierite-garnet-H_2O equilibrium: A geological thermometer, baromater and water fugacity indicator. Contrib. Mineral. Petrol. 77, 38—46.

Marttila, E. 1976. Evolution of the Precambrian volcanic complex in the Kiuruvesi area, Finland. Geol. Surv. Finland, Bull. 283, 109 p.

Marttila, E. 1977. Pre-Quaternary rocks. Sheet 3323, Kiuruvesi. Geological Map of Finland, 1 : 100 000.

Marttila, E. 1981. Kiuruveden kartta-alueen kallioperä. Summary: Pre-Quaternary rocks of the Kiuruvesi map-sheet area. Geological Map of Finland, explanation to the maps of Pre-Quaternary rocks. Sheet 3323.

Mattinson, J.M. 1982. U-Pb "blocking temperatures" and Pb loss characteristics in young zircon, sphene and apatite. The Geol. Soc. Amer., 95th Ann. Meeting, Abstracts with Programs, 14, p. 558.

McLelland. J.M. & Whitney, P.R. 1977. The origin of garnet in the anorthosite-charnockite suite of the Adirondacks. Contrib. Mineral. Petrol. 60, 161—181.

Newton, R.C. 1983. Geobarometry of high-grade metamorphic rocks. Am. J. Sci. 283-A, 1—28.

Newton, R.C. & Wood, B.J. 1979. Thermodynamics of water in cordierite and some petrologic consequences of cordierite as a hydrous phase. Contrib. Mineral. Petrol. 68, 391—405.

Newton, R.C. & Haselton, H.T.I. 1981. Thermodynamics

of the garnet-plagioclase-Al_2SiO_5-quartz geobarometer. *In* Thermodynamics of Minerals and Melts ed. by Newton, R.C., Navrotsky, A. & Wood, B.J. New York: Springer, 129—145.

Newton, R.C. & Perkins, D. 1982. Thermodynamic calibration of geobarometers based on the assemblages garnet-plagioclase-orthopyroxene (clinopyroxene)-quartz. Am. Mineral. 67, 203—222.

Pajunen, M. 1986. Deformation analysis of cataclastic structures and faults in the Tervo area, Central Finland. Geol. Surv. Finland, Bull. 339, 16—31.

Pajunen, M. 1988. Tectono-metamorphic evolution of the Hallaperä pyrrhotite-pyrite ore deposit, Central Finland. Geol. Surv. Finland Bull. 343, 51—76.

Perchuk, L. I. & Lavrenteva, I.V. 1983. Experimental investigation on exchange equilibria in the system cordierite-garnet-biotite. *In* Saxena, S.K. (ed), Kinetics and equilibrium in mineral reactions, New York, Springer-Verlag, 199—239.

Perchuk, L.I., Aranovich, L.Ya. Podlesskii, K.K., Lavrant'eva, I.V., Gerasimov, V.Yu., Fed'kin, V.V., Kitsul, V.I., Karsakov, L.P. & Berdnikov, N.V. 1985. Precambrian granulites of the Aldan Shield, eastern Siberia, USSR. J. Metam. Geol. 3, 265—310.

Perkins, D. & Chipera, S.J. 1985. Garnet-orthopyroxene-plagioclase-quartz barometry: refinement and application to the English River subprovince and the Minnesota River valley. Contrib. Mineral. Petrol. 89, 69—80.

Pigage, L.C. & Greenwood, H.J. 1982. Internally consistent estimates of pressure and temperature: The staurolite problem. Am. J. Sci. 282, 943—969.

Powneeby, M.I., Wall, V.J. & O'Neill, H. St. C. 1987. Fe-Mn-partitioning between garnet and ilmenite: experimental calibration and applications. Contrib. Mineral. Petrol. 97, 116—126.

Salje, E. 1986. Heat capacities and entropies of andalusite and sillimanite: The influence of fibrolitization on the phase diagram of the Al_2SiO_5 polymorphs. Am. Mineral. 71, 1366—1371.

Salli, I. 1969. Pre-Quaternary rocks, Sheet 3312, Pihtipudas. Geological Map of Finland, 1 : 100 000.

Salli, I. 1977. Pre-Quaternary rocks, Sheet 3314, Pielavesi. Geological Map, of Finland, 1 : 100 000.

Salli, J. 1983. Pielaveden kartta-alueen kallioperä. Summary: Pre-Quaternary rocks of the Pielavesi map-sheet area. Geological Map of Finland, explanation to the maps of Pre-Quaternary rocks. Sheet 3314.

Sandiford, M. & Powell, R. 1986. Deep crustal metamorphism during continental extension: modern and ancient examples. Earth Planet. Sci. Letters 79, 151—158.

Savolahti, A. 1966. On rocks containing garnet, hypersthene, cordierite and gedrite in the Kiuruvesi region, Finland. Part I: Juurikkajärvi. Compt. Rend. Soc. geol. Finlande 38, 343—386.

Schreurs, J. & Westra, L. 1986. The thermotectonic evolution of a Proterozoic, low pressure, granulite dome, West Uusimaa, SW Finland. Contrib. Mineral. Petrol. 93, 236—250.

Selverstone, J., Spear, F.S., Franz, G. & Morteani, G. 1984. High-pressure metamorphism in the SW Tauern Window, Austria: P-T paths from hornblende-kyanite-staurolite schists. J. Petrol. 25, 501—531.

Sen, S.K. & Bhattacharya, A. 1984. An orthopyroxene-garnet thermometer and its application to the Madras charnockites. Contrib. Miner. Petrol. 88, 64—71.

Spencer, K.J. & Lindsley, D.H. 1981. A solution model for coexisting iron-titanium oxides. Am. Mineral. 66, 1189—1201.

St-Onge, M.R. 1984. Geothermometry and geobarometry in pelitic rocks of north-central Wopmay orogen (early Proterozoic), Northwest Territories, Canada. Geol. Soc. Am. Bull. 95, 196—208.

St-Onge, M.R. 1987. Zoned poikiloblastic garnets: P-T paths and syn-metamorphic uplift through 30 km of structural depth, Wopmay orogen, Canada. J. Petrol. 28, 1—21.

Thompson, A.B. 1976. Mineral reactions in pelitic rocks. II. Calculation of some P-T-X (Fe-Mg) phase relations. Am. J. Sci. 276, 425—454.

Thompson, A.B. 1982. Dehydration melting of pelitic rocks and the generation of H_2O-undersaturated granitic liquids. Am. J. Sci. 282, 1567—1595.

Thompson, A.B. & England, P.C. 1984. Pressure-temperature-time paths of regional metamorphism II. Their inference and interpretation using mineral assemblages in metamorphic rocks. J. Petrol. 25, 929—955.

Tuisku, P. & Sivonen, S. 1984. Paine- ja lämpötilaolosuhteet Kuhmon vihreäkivivyöhykkeen metamorfoosissa. Arkeeisten alueiden malmiprojekti, raportti n:o 19. Oulun yliopisto.

Vaasjoki, M. & Sakko, M. 1988. The evolution of the Raahe—Laatokka zone in Finland: isotopic constraints. Geol. Surv. Finland, Bull. 343, 7—32.

Ward, P. 1988. Mesoscopic scale structural analysis. *In* Exploration target selection by integration of geodata using statistical and image processing techniques: an example from central Finland, Part I (text) *ed. by* G. Gaál. Geol. Surv. Finland, Rep. Invest. 80, 50—53.

Appendix. Map coordinates of sample localities.

Code	Map sheet	x-coord.	y-coord.	Code	Map sheet	x-coord.	y-coord.
1	3323 12D	7065.42	497.54	33	3323 07D	7046.77	486.71
2	3324 07C	7073.04	485.70	34	3314 09C	7030.80	487.46
3	3323 10C	7042.91	499.19	35	3323 08A	7054.41	482.10
4	3323 01C	7043.54	469.27	36	3323 07C	7042.74	489.64
5	3312 12A	7032.04	454.70	37	3314 08D	7029.90	486.80
6	3312 08B	7028.78	443.33	38	3314 08D	7029.91	486.78
7	3312 08B	7028.98	443.32	39	3314 08B	7027.40	481.52
8	3323 10A	7044.89	492.02	40	3314 08B	7027.46	481.09
9	3323 07A	7043.41	484.38	41	3323 06C	7062.42	477.14
10	3314 09C	7033.95	487.29	42	3323 06A	7062.30	472.67
11	3314 08D	7029.68	487.23	43	3314 02A	7024.24	463.30
12	3314 09A	7030.35	484.68	44	3314 02C	7021.43	468.03
13	3314 08D	7029.73	486.85	45	3314 12B	7035.58	491.90
14	3314 08D	7029.85	486.83	46	3314 09D	7035.04	487.22
15	3323 07A	7042.55	483.98	47	3314 09C	7031.29	488.29
16	3314 08B	7027.40	481.12	48	3314 09C	7030.84	487.44
17	3314 06D	7038.07	476.45	49	3323 07A	7040.70	483.85
18	3323 04C	7043.42	479.10	50	3314 08B	7027.49	481.08
19	3323 05C	7051.34	478.84	51	3323 04B	7049.96	474.47
20	3323 05C	7052.70	477.53	52	3323 05C	7052.05	478.10
21	3323 07A	7043.06	482.18	53	3323 07A	7041.41	483.39
22	3323 02C	7054.70	468.20	54	3323 05C	7051.82	477.07
23	3324 04B	7077.47	472.74	55	3323 07A	7044.64	483.10
24	3323 03D	7069.86	469.64	56	3314 09C	7030.40	487.07
25	3321 10D	7045.39	459.38	57	3323 07A	7042.55	483.98
26	3321 10C	7042.53	456.59	58	3314 08B	7028.10	483.25
27	3312 12A	7031.70	454.70	59	3323 04B	7045.70	474.50
28	3323 07C	7042.42	486.38	60	3323 06A	7060.92	474.36
29	3314 05B	7029.62	473.70	61	3323 07B	7045.55	483.16
30	3321 08D	7056.64	446.84	62	3323 05D	7055.46	476.13
31	3314 03B	7036.31	464.41	63	3314 09A	7031.25	484.76
32	3321 06C	7062.30	439.55	64	3323 08A	7052.62	482.23
				Age det, sample, Mustikkamäki	3314 09D	7038.85	487.20

Tätä julkaisua myy

GEOLOGIAN
TUTKIMUSKESKUS (GTK)
Julkaisumyynti
02150 Espoo

☎ 90-46931
Teleksi: 123 185 geolo sf
Telekopio: 90-462 205

GTK, Väli-Suomen
aluetoimisto
Kirjasto
PL 237
70101 Kuopio

☎ 971-164 698
Telekopio: 971-228 670

GTK, Pohjois-Suomen
aluetoimisto
Kirjasto
PL 77
96101 Rovaniemi

☎ 960-297 219
Teleksi: 37 295 geolo SF
Telekopio: 960-297 289

Denna publikation säljes av

GEOLOGISKA
FORSKNINGSCENTRALEN (GFC)
Publikationsförsäljning
02150 Esbo

☎ 90-46931
Telex: 123 185 geolo sf
Telefax: 90-462 205

GFC, Mellersta Finlands
distriktsbyrå
Biblioteket
PB 237
70101 Kuopio

☎ 971-164 698
Telefax: 971-228 670

GFC, Norra Finlands
distriktsbyrå
Biblioteket
PB 77
96101 Rovaniemi

☎ 960-297 219
Telex: 37 295 geolo SF
Telefax: 960-297 289

This publication can be obtained
from

GEOLOGICAL SURVEY
OF FINLAND (GSF)
Publication sales
SF-02150 Espoo, Finland

☎ 90-46931
Telex: 123 185 geolo sf
Telefax: 90-462 205

GSF, Regional office of
Mid-Finland
Library
P.O. Box 237
SF-70101 Kuopio, Finland

☎ 971-164 698
Telefax: 971-228 670

GSF, Regional office of
Northern Finland
Library
P.O. Box 77
SF-96101 Rovaniemi, Finland

☎ 960-297 219
Telex: 37 295 geolo SF
Telefax: 960-297 289

ISBN 951-690-306-1
ISSN 0367-522X